EFFECTS OF LOW DOSE IONIZING RADIATION ON DNA DAMAGE AND REPAIR RESPONSE IN PROLIFERATING MUSCLE STEM CELLS

By

OLUWASEUN ODEBUNMI

Thesis submitted to the University of Ottawa in partial fulfillment of the requirements for the degree of Master of Science

Department of Biochemistry, Microbiology and Immunology,

Faculty of Medicine

University of Ottawa

ABSTRACT

There is substantial evidence on the carcinogenic properties of high doses of Ionizing Radiation (IR), however, whether such risks exist following exposure to low doses of radiation (LDR) (below 100mGy) remains controversial. The longevity of skeletal muscle stem cells in the body as a "satellite pool" increases their chances of accumulating genotoxic damage from stressors including IR. LDR has been reported to reduce these threats and salvage the health and survival of the skeletal muscle and that of the whole body. Previous studies suggested that muscle myoblasts exposed to LDR (10 and 100mGy) retain their myogenic capacity over a prolonged period of time better than non-irradiated control cells. Therefore, the aim of this study was to determine whether the observed LDR-triggered delay in ageing and functional decline was associated with enhanced genomic stability and error-free Homologous Recombination (HR) repair. To achieve this, mouse (C2C12) and human (HSKM) myoblasts were exposed to 10 or 100mGy of gamma-radiation and grown under optimal conditions for up to 12 (C2C12) or 2 weeks (HSKM). These cells were examined at time points 0, 4, 8 and 12 weeks for function, double-strand breaks (DSB) formation and repair and genomic instability. The results showed the suppression of genomic instability following exposure to LDR and a slight enhancement of HR repair in aged mouse myoblasts. On the other hand, LDR did not affect the generic DSB repair capacity. The unpronounced changes in the human model suggest that responses to LDR vary between species. The variability in the results still leaves a gap as to whether the improved function induced by LDR is associated with better HR activity and may imply alternative DNA repair mechanisms.

ACKNOWLEDGEMENTS

This work would not have been possible without the financial support from the CANDU Owners Group and the permission of Canadian Nuclear Laboratories to undertake this project on their site.

I am grateful to all of those with whom I have had the pleasure to work during this project. Dr. Yevgeniya Le and Dr. Mireille Khacho, both members of my Thesis Committee provided me all of the professional guidance I needed and were always present at my TAC meetings.

I would especially like to thank Dr. Dmitry Klokov, my thesis supervisor. As my teacher and mentor, he has taught me more than I could ever give him credit for here. He believed in me from the very first day and has been a good example and a strong support to me.

To Dr. Tommy Alain, my co-supervisor, thank you for your time, support and guidance. To Dr. Soji Sebastian, thank you for being a part of my project, your expertise, advice and feedbacks are greatly appreciated.

I won't fail to acknowledge Jais Kavumkal for her huge involvement in my project. The successful completion of this project would have been impossible without you. Thank you so much! And to the Radiobiology and Health department at CNL, a big thank you for your patience and dedication. For providing me with the opportunity to learn and practice various laboratory techniques.

I would like to thank my lovely family; whose love and guidance are with me in whatever I pursue.

Above all, I ascribe all the glory to the Almighty God for his merciful operation throughout the entirety of this journey and for bringing me to its end.

TABLE OF CONTENTS

List of Abbreviations

ATCC	American Type Culture Collection
ATM	Ataxia Telangiectasia Mutated
ATR	AT and Rad3-related
BRCA	Breast Cancer Gene
CT	Computed Tomography
DDR	DNA Damage Response
DMD	Duchenne Muscular Dystrophy
DMEM	Dulbecco's Modified Eagle's Media
DNA-PK	DNA-dependent Protein Kinase
DSB	Double Strand Breaks
F.I	Fusion Index
FBS	Fetal Bovine serum
GI	Genomic Instability
H2AX	H2A histone family member X
HDR	High Dose Radiation
HR	Homologous Recombination
HSKM	Human Primary Skeletal Muscle cells

IR	Ionizing Radiation
IRIF	IR-induced Foci
LDR	Low Dose Radiation
LIG IV	Ligase 4
LNT	Linear-No-Threshold
MRN	Mre11, Rad50 and NBS1
MuSC	Muscle Stem Cells
MyH3	Myosin Heavy Chain 3
NHEJ	Non-Homologous End Joining
RF	Replication fork
RNA	Ribonucleic acid
RT-PCR	Reverse Transcriptase-Polymerase Chain Reaction
RNF8	Ring Finger Protein
XRCC	X-ray Repair Cross-complementing Protein
SSB	Single Strand Breaks

List of Figures

List of Tables

CHAPTER 1: INTRODUCTION

1.1: Overview of ionizing radiation and biological relevance

Ionizing Radiation (IR) consists of high energy photons or elementary particles travelling in space and capable of displacing an electron from its orbit causing ionization of atoms and molecules [1]. Damage occurs when an electron displacement happens in the DNA molecule or when DNA hits or interacts with highly reactive hydroxyl radicals formed as a result of the electron's displacement from water molecules [2]. Such damage to DNA may result in single or double strand breaks (SSB or DSB), oxidized bases, inter- and intra-strand crosslinks and others. If DSBs are unrepaired or improperly repaired, they could lead to cell death or cause chromosomal aberrations, that are frequently associated with cancer [3, 4]. There is substantial evidence on the carcinogenic properties of high doses (doses greater than 100mGy) of IR (HDR), but whether risks of cancer exist following exposure to low doses of IR (LDR) remains controversial [5, 6]. To control and regulate exposure of humans to IR, the Linear-No-Threshold (LNT) theory has been adopted by international advisory and regulatory bodies. The LNT model implies a linear increase in cancer risk with any IR dose (Fig 1). Although backed by atomic bomb survivors' data at high doses, the LNT lacked experimental support for the low-dose region. Yet, the LNT has been in use for decades globally [7]. However, many studies have refuted the validity of this model because of its lack of statistical power at low doses, contradictions with the biology of DNA repair and extrapolation from high-dose data to estimate LDR-associated risks [8-10]. The identification of nontargeted effects such as radioadaptive responses (RAR), radiation-induced bystander effects (RIBE) and LDR hypersensitivity add to the uncertainties observed with the LNT model [11-13].

This ambiguity and the growing use of LDR in diagnostic imaging has, in recent years, stirred up interest in the biological effects of LDR and defining thresholds for detectable detriment.

Studies on the effect of LDR on cells have shown a wide range of results due to the variation in cell types, radiation type, and doses [14-17]. Although observed in a great variety of studies [18, 19], radiation adaptive response is not a universal phenomenon and depends on a cell type, biological end-point and radiation qualities [20]. Some studies have shown no effect of LDR on cells [21, 22]. Demonstrated beneficial effects of LDR [14, 15, 23] have been proposed to be mediated via several mechanisms. These include enhancement of DNA repair mechanisms [24, 25], activation of antioxidant systems [26, 27] and some others. It was also shown however that cells may not be able to activate their DNA damage responses at low levels of DSB such as those induced by LDR, adding some controversy to the issue of biological effects of LDR [28]. Given such variability of results it would be difficult to predict biological responses and consequences in poorly investigated cell types that represent potential future targets for medical applications. Muscle stem cells are among such cells.

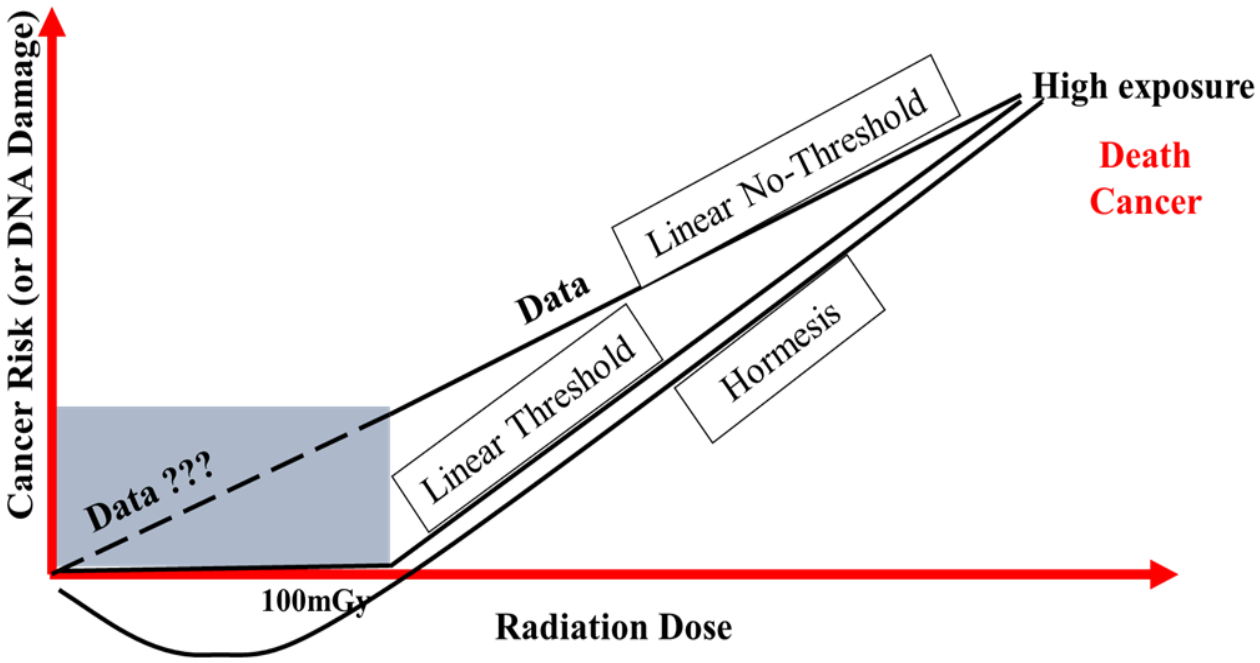
Cancer Risk (or DNA Damage)
High exposure
Death
Cancer
Linear No-Threshold
Data
Linear Threshold
Hormesis
Data ???
100mGy
Radiation Dose

Fig 1: Schematic diagram illustrating various dose-response models in radiation cancer risk assessments: Linear-No Threshold model (LNT) indicating linear relationship between dose and effect, Linear-Threshold (LT) model defining doses of 100mGy and below as risk-free and Hormesis model stating that doses at 100mGy and below are beneficial.

1.2: Ionizing Radiation and DNA damage & repair

1.2.1: DNA damage and repair overview

Exposure to IR induces a variety of DNA lesions, including base damage, base release, depolymerization, crosslinking, SSB and DSB [29]. Among them, DSB is the most critical lesion, which when unrepaired or incorrectly repaired, can lead to genomic instability or cell death. Cells have evolved two main pathways to repair these lesions: the error-prone non-homologous end-joining (NHEJ) pathway, that ensures direct resealing of DNA ends; and the accurate homologous recombination (HR) pathway that relies on the presence of homologous DNA sequences for DSB repair [30]. Previous studies have identified different proteins involved in DSB repair [31-35] and these proteins have been categorized based on their critical involvement in damage recognition and signalling, checkpoint implementation and repair [36].

1.2.2: DNA damage signalling and checkpoint

Cellular response to genotoxic stress is a complex process and usually starts with the sensing of DNA damage. The large Ataxia Telangiectasia Mutated (ATM) and AT and Rad3-related (ATR) kinases have come into focus as early, central participants in the DNA damage recognition and signaling processes [37,38]. Upon induction of DSB, ATM undergoes auto-phosphorylation leading to the formation of high density of phosphorylated ATM in the vicinity of each DSB [39]. Activated ATM then phosphorylates histone H2AX (modification referred to as γH2AX) [31], DNA-PK and ATR also contribute to this modification under certain conditions [40, 41]. ATM phosphorylates numerous other key proteins that often appear in the nucleus as foci and mediate checkpoints and DNA repair. The formation of γH2AX is one of the earliest events at a DSB, and this mark spreads

over at least a megabase of chromatin adjacent to each DSB in mammalian cells [42]. Although γH2AX is not essential for the initial recruitment of DSB response factors, it plays a significant role in the retention of repair factors, chromatin conformation and in DNA damage checkpoint [43]. In addition, γH2AX is the most common marker of DSB [44]. Also, using Next Generation Sequencing (NGS) methods the genome-wide distribution of DNA damage hotspots was uncovered by loci specific γH2AX [45]. *In order to measure DNA damage response, two proteins: phosphorylated ATM and H2AX will be used as DSB markers in this study.*

1.2.3: Double Strand Breaks repair pathways

Cells have evolved two mechanistically distinct pathways to eliminate DSB from the genome. The first repair pathway, NHEJ, is known for its predominance throughout the cell cycle and accounts for nearly all DSB repair outside of the S and G2 phases [46]. 53BP1 is a key DNA repair factor that promotes NHEJ and plays a vital role in defining DSB repair pathway choice in the G1 and S/G2 phases of the cell cycle [30, 47, 48]. The NHEJ is the major repair pathway in G_1 cells due to lack of sister chromatids for HR [49, 50]. Double-strand break repair by NHEJ is accomplished by a direct ligation of the two broken DNA ends. The initial end recognizing components of the NHEJ pathway, the Ku70–Ku80/86 (Ku) heterodimer and the DNA dependent protein kinase catalytic subunit (DNA-PKcs), act in concert with ATM, Mre11, Rad50 and NBS1 (MRN complex), MDC1, ring finger protein 8 (RNF8), E3 ubiquitin-protein ligase) and XRCC4 x-ray repair cross-complementing protein 4 (XRCC4) –LIG4 ligase 4 (LIG 4) complex [4, 51] (Fig 2).

The second DSB repair pathway is HR, that unlike NHEJ requires a homologous template and is initiated by DNA 5′-end resection [52]. RAD51 is central to HR, as it mediates pairing of

homologous DNA sequences and strand invasion [53]. It functions by forming nucleoprotein filaments in single-stranded DNA, mediating homologous pairing and strand exchange reactions between single and double stranded DNA during repair [54]. The choice between HR and NHEJ depends primarily on the cell cycle stage and the nature of the break. During the G1 phase, HR is inactivated and NHEJ is dominant, but during the S and G2 phases, when sister chromatids are available, NHEJ and HR compete [55].

Although it is reported that stimulation of DNA damage response by LDR triggers radio-adaptive response [12, 56], the involvement of exact DNA repair pathway and its role is not clear yet. There are reports that have demonstrated that exposure to IR induces DSB of which ~80–90% are rejoined in G_0/G_1 in a manner dependent upon the NHEJ core components, that is, Ku, DNA-PKcs, XRCC4 and DNA Ligase IV [57]. Some other studies showed that NHEJ initially attempts to repair DSB in G2 (at two-ended DSB, which are directly induced by IR); furthermore, if NHEJ does not ensue, the repair pathway switches from NHEJ to HR due to DNA damage or chromatin complexity [58]. End resection, which promotes HR, is inhibited by the DNA repair-associated proteins RIF1 and 53BP1 during G1, thereby restricting HR activity to S and G2 [31, 59, 60].

While some studies suggest that NHEJ is a more efficient DSB repair pathway than HR because of its faster kinetics [61, 62], some others suggest the reverse [63, 64]. It is however important to note that each repair mechanism has its distinct role in securing the genome. NHEJ is flexible and proficient in dealing with a wide range of DSB over a short time [65], whereas, HR dynamics involves more complex interactions, takes longer to process damage, but is however accurate when repair is initiated [66].

Therefore, to measure the efficiency of each repair type, two important factors must be considered: 1) the ability to complete repair process by eliminating most damage induced by exposure, and 2) the maintenance of chromosome stability. Both parameters will be measured in this study.

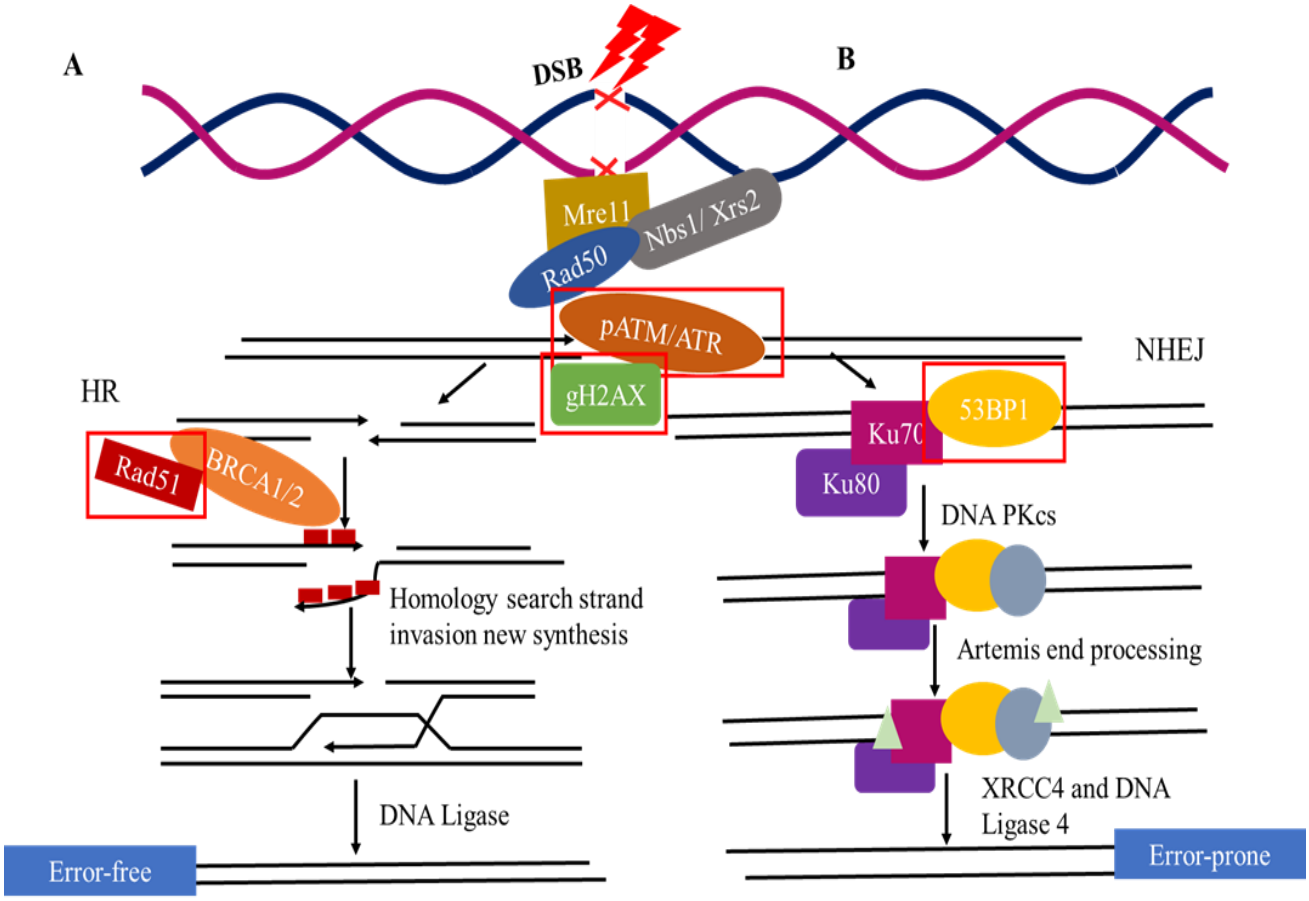
A
DSB
B
Mre11
Nbs1/ Xrs2
Rad50
pATM/ATR
gH2AX
HR
NHEJ
Rad51
BRCA1/2
53BP1
Ku70
Ku80
DNA PKcs
Homology search strand invasion new synthesis
Artemis end processing
XRCC4 and DNA Ligase 4
DNA Ligase
Error-free
Error-prone

Fig 2: DNA double strand break repair pathways. A: Homologous recombination (HR) repair. Mre11-Rad50-NBSI (MRN) complex recognizes and senses double strand breaks (DSB). In response to that, ATM is activated and phosphorylates H2AX protein. The end resection from 5' to 3' is performed by the nuclease which leads to the formation of single stranded DNA (ssDNA). Rad51 nucleoprotein filament is assembled to perform homology sequence searching and mediate strand invasion. Repair is completed by ligation and resolution of holiday junctions; B: Non-homologous end joining (NHEJ) repair. The two broken ends are processed and ligated directly by the action of the end-binding KU70/80 complex and DNA PKcs followed by binding of the 53BP1 protein and by ligation by XRCC4-ligase 4. *The proteins boxed in red: pATM and γH2AX, 53BP1 and Rad51 were used in this study as markers of DSB, NHEJ and HR repair respectively.*

1.3: DNA repair and Genomic Instability

1.3.1: Overview

DSB are cytotoxic lesions, which if left unrepaired, lead to severe unwanted consequences, such as loss of genetic information, chromosomal rearrangements and even cell death [67]. Cells have evolved conserved recombination mediated genome editing pathways as a means of repairing DSB and restarting replication forks, thus allowing genome duplication to continue [68]. The lack of repair, as well as defects could result in the deletion or insertion of the genetic information and introduce the risk of neoplastic transformation. These changes could get transmitted and accumulate in the cell's progeny. Inability to maintain the integrity of DNA and chromosomes is called genomic instability (GI). To determine whether repair in a cell is efficient, the delayed effects of a stimulus on a genome must be assessed.

1.3.2: NHEJ and GI

NHEJ repair pathway involves the use of fast mechanisms to rejoin broken ends but has for long been considered error-prone and known to be mostly associated with a higher frequency of chromosomal aberrations. Although, a few studies have suggested certain components of NHEJ like Ku, XRCC4/Lig IV proteins might have a caretaker role in maintaining genomic stability [69-72], certain others show evidence of its fallibility and proof of its frequent association with the presence of small insertions and deletions (indels) at the break site [73-76], which can lead to mutations. NHEJ-mediated defects result in increased sensitivity of cells to genotoxic agents including IR. Cytological studies in Fanconi Anemia cells show that the vast majority of radial chromosomes generated in response to DNA cross-links arise as a result of translocations between non-homologous chromosomes, which is a signature of repair by NHEJ [77, 78]. In a study by K. Mujoo et al., a high

frequency of residual γ-H2AX foci was observed in differentiated embryonic stem cells and an accumulation of RIF1 at DSB sites containing phosphorylated 53BP1 [79]. In the same study, where NHEJ was dominant in differentiated embryonic cells, increased residual/unrepaired DSB were observed to correlate with a high level of chromosomal aberrations [79]. Also, the inactivation of BRCA2, a protein required for Rad51 function [108], in HeLa cells increased nuclear fragmentation frequency and caused high rates of chromosomal aberrations, including gaps/breaks, radial chromosomes, and translocations, after DSB induction. Unlike BRCA2, inactivation of DNA ligase 4 or XRCC4 alone had no appreciable effect on nuclear integrity after IR treatment and genetic ablation of key NHEJ components did not fully suppress the BRCA2-associated deficits. This implied that repair by NHEJ amongst other DSB repair pathways contributed to the gross GI observed in BRCA2-depleted cells after DNA damage [80].

1.3.3: HR and GI

HR is the process by which DNA molecules of identical or nearly identical nucleotide sequences interact and exchange information that may or may not result in rearrangement of genetic information [81]. Notable for its homology sequence and resection mechanism, HR compared to the error-prone NHEJ, is known to be the most-precise repair mechanism. In a study by C. Wiese et al., human cells depleted for Rad51 associated protein-1 were hypersensitive to chromosomal lesions including DNA crosslinks [82]. HR plays a pivotal role in the resumption of stalled replication forks (RF) and defects in HR lead to spontaneous slowed replication fork progression, anaphase bridges, common fragile sites, and supernumerary centrosomes, which result in multipolar mitosis and aneuploidy [83]. RF deceleration and chromatin bridges at anaphase were observed in cells affected by a loss of function mutation in the endogenous BRCA2 gene (VC-28 cells) and cells that express

a dominant negative form of Rad51 (V79SM24) [84]. These data underline the essential role played by HR in protecting genome stability at the interface between replication and mitosis.

Therefore, in this study it was examined whether LDR can protect the fidelity of the DNA homeostasis, including at longer times after exposure, by differentially activating one or another type of DSB repair pathway. Such influence would affect genomic stability and is a largely unexplored topic in radiobiology of stem cells.

1.4: Effects of LDR on DNA damage response

Irradiation of cells elicits a complex response. While the consequences of irradiation with high doses (>100mGy) have been the subject of considerable attention, less is known about the response to low doses (<100mGy). Studies are still ongoing on the choice of repair pathway promoted by LDR: HR or NHEJ. Certain studies have shown that LDR enhances error-free HR repair [85, 105]. LDR-specific genome-wide gene expression profiles from GEO microarray datasets identified increased levels of Rad51 protein in 10mGy-irradiated hepatocytes [85]. Studies have shown that priming cells with LDR increases radioresistance and decreases chromosomal aberrations resulting from subsequent exposures to high-dose IR ("challenge IR"), a phenomenon referred to as the adaptive response. A recent report showed that chronic LDR treatment promotes HR, as demonstrated by an HR reporter assay [86]. The observation of high rates of HR following LDR is consistent with the notion of increased radio-resistance in radio-adaptive responses. Although it is evident that priming LDR promotes the usage of HR in somatic cells, it remains unclear if it does the same in stem or progenitor cells.

To better understand this, the study is aimed towards determining the effects of low dose ionizing radiation on DNA damage and specific DSB repair pathways in stem cells.

1.5: Stem cells and their responses to LDR

1.5.1: Stem cells and current knowledge on the beneficial effects of LDR on stem cells

Stem cells are fundamental components of biological organization, responsible for the homeostatic maintenance of mature and functional tissues and organ systems. They divide and renew for long periods to replenish dying cells and regenerate damaged tissues throughout an organism's lifetime. Regenerative medicine involving the use of stem cells as therapies has been extensively investigated using the regenerative properties of stem cells for the treatment of various diseases [87, 88]. Assessment of stem cell transplants, their survival and treatment efficacy frequently use the form of diagnostic radiology procedures such as computed tomography (CT) scans, X-rays, nuclear medicine and fluoroscopy [89]. Evaluation of the effects of LDR is a medical and social issue for the health of patients who undergo CT imaging for diagnosis [90] since the fate of cell engraftment, survival and proliferation following exposure to LDR from imaging techniques has been evasive. Many studies suggest that LDR might have beneficial effects on cellular response in different stem cells. In a study by X. Liang et al., exposure of rat mesenchymal stem cells to LDR enhanced the phosphorylation of the Raf-MEK-ERK pathway proteins, known for their role in improving cell cycling and proliferation [91]. Similarly, bone marrow mesenchymal stem cells exposed to X-ray doses below 200mGy displayed enhanced proliferative ability as compared with the control group [92]. In addition to *in vitro* studies, *in vivo* experiments that focused on the effect of LDR in stem cells have also been performed. In a study by G. Wang and L. Cai, low dose X-rays stimulated bone

marrow stem cell proliferation and peripheral mobilization in adult Kunming mice [56, 93] and induced accelerated skin wound healing in diabetic rats [94].

There have been significant advances in our understanding of the molecular mechanisms of radiation induced DNA damage and the cellular responses occurring after such insult. An important issue in the radiation sciences is whether LDR can stimulate the repair process and whether the beneficial effects manifested at the cellular level are associated with this process [95].

1.5.2: Effects of LDR on DNA damage response in stem cells

Stem cells (SCs), given their long lifespan, can accumulate damage due to intrinsic and extrinsic stress including exposure to radiation. They can experience DNA replication errors and accumulate mutations thereby inducing tumorigenesis [96]. For this reason, they possess a powerful and effective DNA repair system to properly fix DNA damage and avoid the onset of pathologies, such as cancer or aging related disease [97]. Emerging evidence suggests that SCs do indeed respond to DNA damage differently compared to their somatic counterparts. A study by K. Jacobs et. al., examining the relative radio-sensitivity of undifferentiated SC populations compared with differentiated non-SC showed normal SCs were more radiosensitive, whereas non-SCs were highly radioresistant and only underwent minimal apoptosis even at high doses. This study showed that undifferentiated normal SCs exhibited persistent phosphorylation of H2AX-Y142 along the DNA breaks, thus promoting apoptosis while inhibiting DDR signaling and DNA repair [98]. However, these findings might not be applicable to all SC populations across every tissue niche. Indeed, relatively high radioresistance of SCs has been reported in some tissues [99, 100].

The frequency of mutations in embryonic stem cells (ESCs) is lower than in differentiated cells because of an efficient DNA repair [101]. Scientists demonstrated that ESCs spend roughly 70-75% of their lifecycle in S-phase when the HR is active [102]. In a model of induced DSB by the conditional expression of an endonuclease, Francis and Richardson showed that somatic cells repair DNA either by HR or NHEJ, while in ESCs the activity of NHEJ is negligible [103]. The stability of the ESC genome is highly desirable because a mutation can have profound consequences on the organism's development.

DNA damage and repair in adult stem cells has not been fully investigated. Previous studies have shown that adult stem cells from various tissues may have specific DNA repair mechanisms for DSB [104]. A study on spermatogenic stem cells exposed to 100mGy X-rays reported high levels of 53BP1 2h following irradiation [105]. This study, however, did not specifically investigate HR repair activity in the cells.

The exposure of mesenchymal stem cells to prolonged X-ray irradiation of 270mGy/h revealed a linear accumulation of Rad51 foci between 2 and 6h of irradiation [106]. This implies a higher activity of HR, which can be monitored by the expression of Rad51 proteins [53]. Similarly, mesenchymal stem cells exposed to 100mGy displayed elevated levels of mRNA transcripts of the BRCA1 and BRCA2 genes 30 minutes post-irradiation [107]

Understanding intricate details of responses to radiation exposures in various types of SCs is currently an active area of research. *In this study, we sought to examine the effects of LDR on DNA damage and repair in proliferating muscle stem cells.*

1.6: Muscle stem cells (MuSC), LDR and Aging

1.6.1: MuSC overview

Muscle stem cells, also known as satellite cells, are undifferentiated tissue-specific stem cells located between muscle fibres and the basement membrane ensheathing it [109]. Satellite cells are activated and proliferate in response to stimuli and simplistically, have two main fates—to return into quiescence and repopulate the satellite cell niche, or differentiate to regenerate or repair muscle fibers [110]. The maintenance of reversible quiescence in satellite cells and their activation are thus essential for efficient tissue homeostasis and regeneration. In response to repeated muscle tissue injury throughout life, reconstitution of the damaged tissue is coordinated with the maintenance of a healthy stem cell population that can continue to ensure optimal tissue homeostasis [111].

1.6.2: Effects of LDR on aging in MuSCs

Aging is an inevitable physiological consequence of living organisms that occurs over time [112]. Stem cells are characterized by their ability to reside in the body for long periods, self-renewal and differentiate into various cell types. However, their renewal and functional ability deteriorates as they age.

The regenerative properties of muscle stem cells are recognized as remarkable but are similarly not protected from declining with age [113]. Muscle function can be impaired as a result of different external and internal conditions such as trauma, disuse, disease states or as a result of aging. Aging diminishes the regenerative capacity of skeletal muscle in multiple ways, compromising recovery after injury [114]. This is driven primarily by the functional decline in tissue-resident stem cell

populations. In skeletal muscle, the resident stem cell population, SCs are numerically and functionally compromised with aging, and the microenvironment (the niche) of the SC becomes less supportive [114]. Previous studies have reported the effects of low dose irradiation on the longevity and survival of insects [115, 116] and animals [117, 118]. Humans have also displayed anti-aging properties following exposure to LDR. For example, better survival and other beneficial effects of low doses of atomic bomb radiation were reported for Hiroshima and Nagasaki survivors [119, 120]. Similarly, mortality rates of all workers in UK's Atomic Energy Authority were found to be lower than national rates [121]. All-cause mortality and all-cause cancers (leukaemia and prostate cancer) were also significantly lower for nuclear workers than for non-radiation workers [121]. On the contrary, an epidemiologic study reported several health problems, such as increased risk of skin cancer and leukemia along with enhanced cancer and all-cause mortality rates were found in radiologic technologists and radiologists in the first half of the past century [122]. In the case of stem cells, a conference abstract showed evidence of delayed aging in mesenchymal and endothelial stem cells [123]. To date, only one study that examined the effects of LDR on muscle stem cells has been published [124]. Findings from this study showed that the proliferation, differentiation and self-renewal of satellite cells were unaffected by LDR at the acute phase but displayed a slight reduction of proliferative ability in LDR-exposed mice at the chronic phase.

1.6.3: Diseases associated with MuSC functional deficit

Satellite cells as a population are primarily quiescent, dividing very infrequently under normal conditions in the adult. Several lines of evidence suggest that quiescence is not merely an inactive basal state, but rather is a state under active transcriptional control [125]. Once activated, muSCs proliferate and their progeny progress down the myogenic lineage pathway to become fusion-competent myoblasts. [126, 127]. However, this regenerative capacity is not unlimited, as exhaustion

of the satellite cell population is an important factor in the deterioration and the existence of functional decline-associated diseases. Many factors could contribute to this depletion, one of which is age. In skeletal muscle, aging is manifested by the loss of SCs [128]. Satellite cells present reduced capacity for self-renewal leading to sarcopenia [129, 130]. These age-related degenerative losses of muscle mass, quality, and function take place in the absence of any underlying disease. Skeletal muscle is eventually replaced by fatty and fibrous tissue, which results in functional impairment of the muscle and hence, physical disability. In some cases, as in muscular dystrophies, certain genes become mutated and thus compromise satellite cells function leading to degeneration and subsequent substitution with adipose/ connective tissues [131]. These diseases create enhanced vulnerability to mechanical stress and subsequent loss of muscles. Satellite cells in children with Duchenne Muscular Dystrophy (DMD) may have the remaining growth capacity as low as might be found in those in their eighth decade of life [132, 133]. Another common factor, which compared to the other two is artificially induced, is cancer therapy. All cancer patients are generally exposed to several cancer-specific and non-cancer-specific factors causing decreased muscle mass and muscle dysfunction, a condition widely known as muscle cachexia [134]. Cancer therapy could affect skeletal muscle change in many ways. Sarcopenia has been found to be prevalent in advanced cancer patients [135].

Stem cell transplantation is one of the methods expected to effectively treat DMD. Many recent studies have used stem cell transplantation to treat DMD in a rat model, with improvements in pathology, physiology, biochemistry, dystrophin expression and motor function [136]. Stem cell transplantation for DMD may involve bone marrow stromal cells, hematopoietic stem cells, or muscle stem cells. Following transplantation, patients undergo repeated diagnostic imaging that exposes them to low doses of ionizing radiation. *This study would help shed light on the effects this exposure would have on the transplanted stem cells.*

1.7: Measurements of DSB repair kinetics

When DSB are produced by IR, it is possible to visualize and analyze the accumulation of DNA damage response and DSB repair proteins by either immunofluorescence microscopy of fixed cells [137] or by fluorescent tagging of various DSB response proteins in live cells in real-time [138]. Under a microscope, these proteins aggregate around each DSB and can be visualized as individual fluorescence spots called repair foci, or in the context of IR exposure: IR induced foci or IRIF [139]. The changes in kinetic behavior of IRIF over a period of time (e.g. 24h) following IR exposure can provide valuable information on their involvement in specific DNA repair pathways and the efficiency of repair as determined by the elimination of foci over time. In this project, aging myoblasts were exposed to high challenging doses of IR to measure DNA repair capacity after prior exposure to low doses. This repair capacity was determined using the principle of repair kinetics. The DSB repair kinetics follows a biphasic pattern: most of the DSB get repaired by the fast component of repair within the first two to six hours after induction, while the remaining DSB can be repaired by the slow component of repair, which acts with slower kinetics and might require several hours –or even days– to complete repair [140-142] (Fig. 3). Regardless of the phase of repair, foci disappearance with time is expected if repair is efficient.

Principle of Repair Kinetics

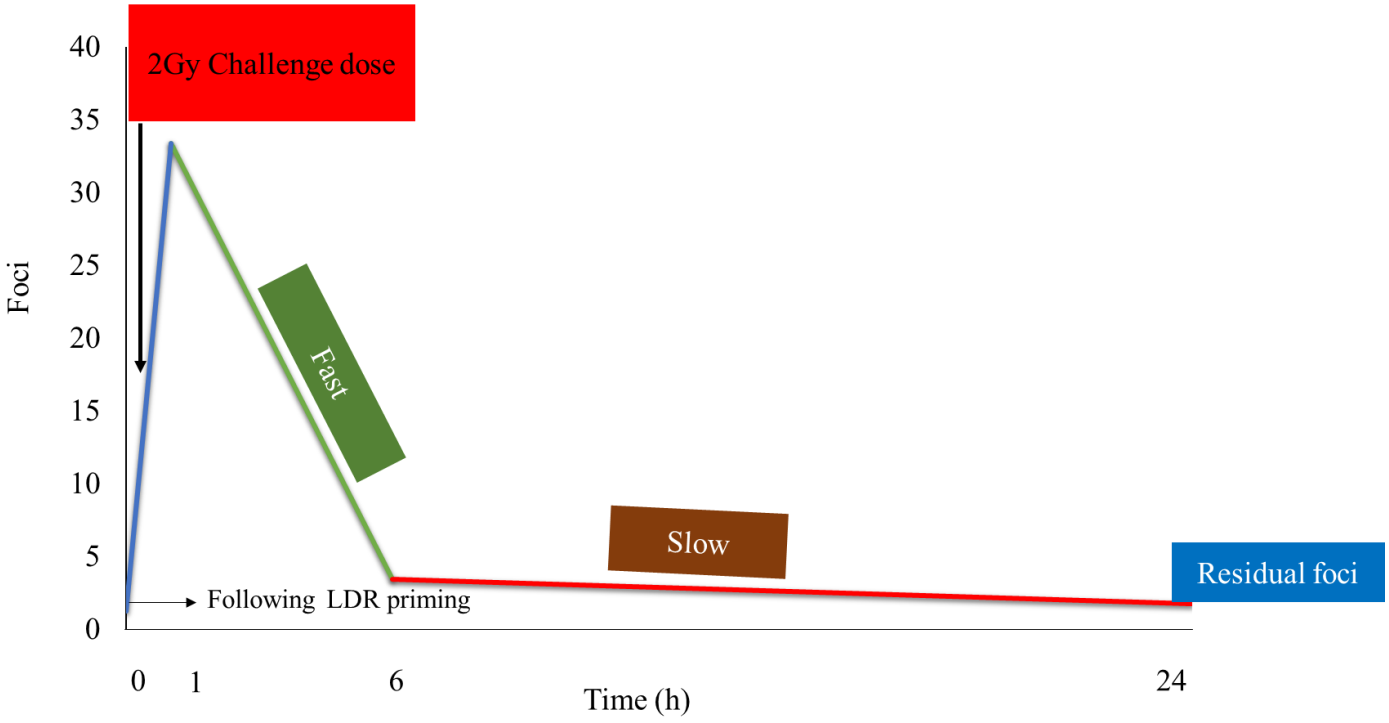

Fig 3: Schematic diagram illustrating the principle of a DSB repair kinetics experiment. Exposure to a high challenging dose at time=0h induces DSB that are visualized by immuno-labeling for DSB repair proteins as foci and quantified. Quantifying foci at different time points post-challenge allows for reconstruction of the repair kinetics since elimination of foci signifies rejoining/repair of DSB. Typically, DSB repair kinetics is measured within 24h by which time the number of residual foci is indistinguishable from untreated control values, if repair is efficient. The slope of the repair curve can be used as an indicator of repair rate, with fast and slow components being distinct from each other. Following this principle, DNA DSB repair was monitored in this study by quantifying foci at time points 0, 1, 6 and 24h post-2Gy challenge.

1.8: Hypothesis, Objectives and Implications

1.8.1: Hypothesis

Aging is a major risk factor for neurodegeneration, cancer, and other chronic diseases [143]. No single molecular mechanism appears to account for the functional decline in different organ systems in older humans, however, one dominant theory is that molecular damage, including DNA damage and mutations, accumulate over time, and that this damage has phenotypic consequences in adult organisms [144]. This is consistent with accumulating evidence that DNA repair pathways and other components of the DNA damage response play a role in preventing neuropathology [145, 146].

Given the previously demonstrated benefits of LDR priming as seen by delayed aging of LDR-exposed cells, it is intriguing to examine whether this effect may be mediated by an LDR-triggered enhancement of DSB repair capacity. Preliminary studies on the effects of LDR on muscle stem cells (MuSC) have shown delayed aging and functional improvement of age-related decline in MuSC. Since it has been shown that aging is associated with the accumulation of genomic instability markers, such as higher rates of DSB in MSC [147], it is feasible to suggest that the beneficial effects observed, as the improved myogenic capacity of LDR-treated myoblasts, may be associated with improvement of DNA damage related responses and the resulting longer retention of genomic stability.

My hypothesis driving this research was the following:

LDR results in preferential and long-term activation of HR DSB repair pathways resulting in enhanced genomic stability and a subsequent improvement of myogenic function in the aging MuSC.

1.8.2: Objective and specific aims

The objective of this study was to investigate DNA damage and DSB repair responses in MuSC exposed to LDR in relation to a decline in their myogenic function with age.

The hypothesis was tested in the following specific aims:

1) to measure how myogenic function of aging myoblasts changes, following exposure to LDR at a young age, and to examine whether correlation with genomic instability exists. LDR-exposed cells will be stimulated to differentiate into muscle fibers at the same time-points GI is measured.

2) to measure how genomic instability in aging myoblasts changes, following exposure to LDR at a young age, and to examine whether correlation with the DSB repair responses exists, basal rate (without high-dose radiation challenge) of DSB, micronuclei and anaphase bridges will be measured as markers of genomic instability.

3) to investigate how DSB repair kinetics curves change in aging myoblasts after exposure to LDR at a young age. The impact of LDR on DSB repair will be determined by exposing aging myoblasts to high-dose radiation challenge and IR induced foci for markers of both HR and NHEJ will be used to construct corresponding repair kinetics curves.

1.8.3: Implications of Research

The significance of this investigation is two-fold: The first is related to regulation of human exposure to LDR: if an improvement of DNA repair and genomic stability with age following LDR exposure

is found, and if this correlates with the functional myogenic improvement, then it would provides useful information to the radiation protection system for better protection of humans from LDR.

The second is the impact it would have on stem cell therapies. In recent years, there has been series of clinical trials on the application of stem cell therapies in the treatment of diseases like Duchenne Muscular Dystrophy. However, the success of this method also rests on the viability of the cells following transplant. Patients would have to undergo repeated examination that would involve exposures to LDR during CT scans. Therefore, understanding the effects of LDR from medical procedures on the transplanted cells would facilitate development and implementation of such therapies

CHAPTER TWO: MATERIALS AND METHODS

2.1: Cell types and Growth media

2.1.1: Skeletal Muscle Myoblasts Cell culture

C2C12 Young Skeletal Myoblasts, strain C3H, Passage 5 were obtained from ATCC CRL-1772. Cells were cultured in Dulbecco's Modified Eagle's Media (Gibco by Lifetech, Grand Island, NY, USA) supplemented with 10% Fetal Bovine serum (FBS) [ATCC, Manassas, USA] and 1% sodium pyruvate at 37^{o}C and 5% CO_2 in air.

2.1.2: Human Skeletal Muscle Myoblasts Cell culture

CC-2580 Normal HSKM, 0Y, female, Lot no. 0000542368 was obtained from Lonza Bioscience. Cells were cultured in Skeletal Muscle Growth Media-2, Single Quots (a constitute of the basal media and supplements: 0.1% human Epidermal Growth Factor, 0.1% Gentamicin-1000, 0.1% Dexamethasone, 2% L-Glutamine and 10% FBS) [Lonza, Walkersville, USA] at 37^{o}C and 5% CO_2 in air.

2.2: Plating Cell Density Optimization

When observed to be 80-90% confluent, cells were passaged on weekdays at 1/10th of the original density and 1/30th the total concentration on weekends. To passage cells, media was aspirated from confluent cultures and the cells were washed once with 1X phosphate buffered saline solution (PBS), without Ca and Mg [Lonza, USA]. The colonies were subsequently treated with 1ml and 2ml of TryplE Express, a dissociation enzyme, on 10mm and 25mm plates respectively, or 0.25% Trypsin-

EDTA (Gibco by Lifetech, Grand Island, USA), in the case of HSKM, for 5 minutes in the incubator. Afterwards, cells were examined to ensure they had detached from the surface of the plate and 9ml/18ml of fresh growth media was added to the plate. The cells were mildly titrated with a glass pipette to break up the clumps and the intended seeding density volume were taken out to re-plate onto 100 x 20mm tissue culture dishes (Corning, USA, NY 14831) in their respective growth media. Each of the three lines of C2C12 was plated at seeding densities ranging from 2×10^4 to 6×10^4 cells and placed in a CO2 incubator overnight. The cells were monitored after 24 hours for viability (ratio of attached vs floating cells), appearance (amount of cell-to-cell contact, 3D formation/clusters) and confluence.

2.3: Irradiation type, Doses and Dose rates

Cobalt-60 was used as the source of gamma irradiation and cells were exposed to sham-irradiation (0Gy), 10mGy and 100mGy (low doses) and 2000mGy (high dose) at dose rates of 0.7 mGy/sec and 32.6 mGy/sec for low and high doses respectively.

For irradiation, Sub-confluent exponential cultures of myoblasts were harvested using trypsin and cultured as a single cell suspension at a density of 10^5 cells/ml in DMEM media containing 1.3% methyl cellulose, 20% FBS, 10 mM HEPES, 200mM L-glutamine and Penicillin-streptomycin antibiotics. After 48 h, when >98% of cells have arrested, suspended cells were harvested by dilution with PBS and centrifugation (Milasincic et al., 1996; S. Sebastian et al., 2009). Arrested cells were reactivated into the cell cycle by replating at a density of 4×10^5 cells per 60 mm dish or 10000 cells on coverslips in GM and harvested at 6-24 h after activation. Under these conditions, myoblasts

enter G_0 and 48 h after suspension culture and upon replating, rapidly and synchronously undergo a G_0-G_1 transition. After attachment, 6 h are required to enter G1and S phase peaks at 20-24 h. This step is essential to mimic the state of stem cells during potential real-life human exposures to LDR. Cells were then washed in PBS to get rid of the cellulose, transferred to DMEM and seeded on 60 x 15 mm plates [Falcon, Durham, USA] for treatment with gamma-radiation. Cultures of irradiated myoblasts were returned to normal growth conditions and used in the assays as described in Fig. 4.

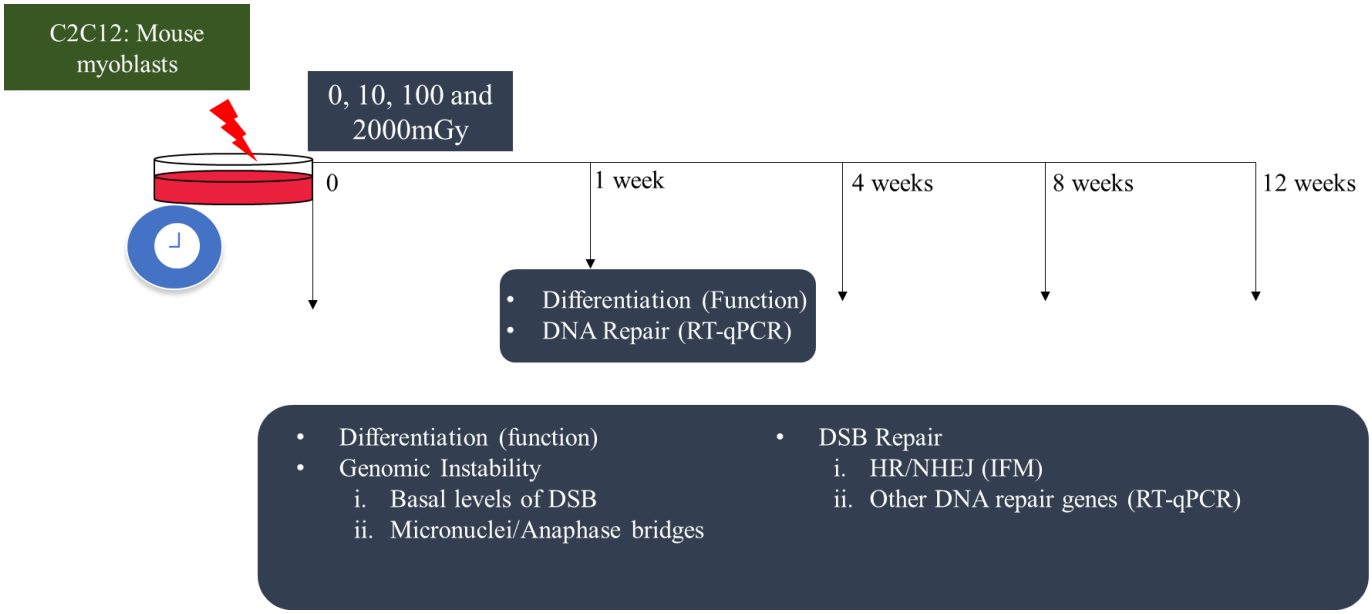
C2C12: Mouse myoblasts
0, 10, 100 and 2000mGy
0
1 week
4 weeks
8 weeks
12 weeks
• Differentiation (Function)
• DNA Repair (RT-qPCR)
• Differentiation (function)
• Genomic Instability
i. Basal levels of DSB
ii. Micronuclei/Anaphase bridges
• DSB Repair
i. HR/NHEJ (IFM)
ii. Other DNA repair genes (RT-qPCR)

Fig 4: Design of the study using mouse C2C12 myoblasts. Quiescent cells were exposed to various doses of gamma-radiation and released from quiescence and maintained by regular subculturing under normal conditions. At time points 0, 4, 8- and 12-weeks post-IR, cells were assessed for myogenic functionality, genomic instability, DNA repair gene expression and DSB repair capacity (using the challenging dose principle). At an earlier timepoint of 1 week, only myogenic functionality and DNA repair gene expression were measured.

HSKM: Human Primary myoblasts

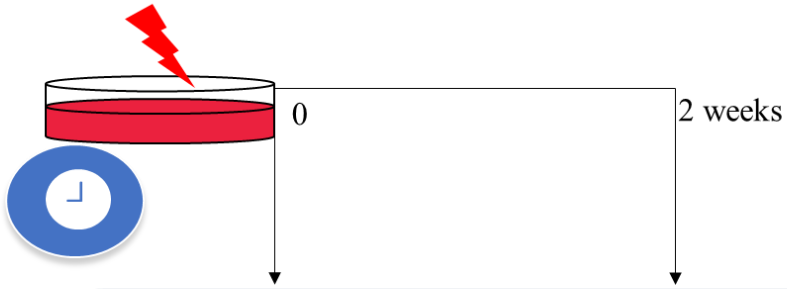

- Differentiation (function)
- Genomic Instability (IFM)
  i. Basal levels of DSB
  ii. Micronuclei (IFM)
- DSB repair
  i. HR/NHEJ (IFM)

Fig. 5: Design of the study using primary human myoblasts. Due to the limitation of this model related to the cells' limited proliferating capacity, one time point of 2 weeks post-irradiation was used. The limitation also resulted in inability to perform DNA repair gene expression analyses and anaphase bridge scoring for genomic instability. The rest of the assays were like in the C2C12 cells study.

2.4: Detection of DSB and their repair

2.4.1: Recognition of DSB

γH2AX and pATM foci were used as markers of DSB. DSB were detected at various time-points: 0, 4, 8 and 12 weeks (mouse samples) (Fig. 4) and 0 and 2 weeks (human samples) (Fig. 5) after initial exposure to doses of 0, 10, 100 and 2000mGy gamma-radiation at t=0h. DSB repair was assessed by using a high-dose challenge to induce substantial number of DSB and monitoring of their repair in the 24h period post-challenge. The principle of DSB repair kinetics experiment is shown in Figure 2. Briefly, 2 x 10^4 cells were grown on glass coverslips in P30 dishes for 24 hours and exposed to the experimental IR doses.

2.4.2: Staining procedure for myoblasts (human and mouse)

Myoblasts were grown on 18" x 18" coverslips [Fisherfinest Premium, Pittsburgh, USA] for 24h and fixed in 2% paraformaldehyde at room temperature (RT) for 30 minutes at time points 0, 1, 6 and 24 h post challenge irradiation (mouse samples) and 0, 1 and 24 h (for human samples) and stored in 1X TBS (10% 10X TBS (10NHCl [36.46 M.W/P.M, Fisherbrand, USA], 500g NaCl [Fisher Scientific, USA], Tris Base [Fisher Scientific, Fair Lawn, NJ, USA], 500g KCl [Fisher Scientific, USA] in RO H20, pH 7.4) at 4ºC until immunofluorescence (IFM) staining. Fixed cells were incubated in -20oC methanol for 60secs for permeabilization of the cells, washed with 3ml of TBS and incubated in TTN (1% Bovine Serum Albumin, pH 7 [Sigma-Aldrich, USA], 0.2% Tween 20 [Sigma-Aldrich, St louis, MO, USA] in TBS to block non-specific binding. Afterwards, cells were stained with primary antibodies, pATM or γH2AX [EMD Millipore Corp, USA] at concentrations of 1:600 & 1:200 respectively and incubated at 4ºC overnight in a humid chamber to

avoid evaporation. Prior to secondary staining, cells were treated with TTN for 10 minutes and washed twice for 5 minutes each with TBST (0.2% Tween 20 in TBS) to decrease background staining and enhance reagent staining. This step was followed by incubation with Goat Anti-Mouse Alexa-488 [Invitrogen by Thermofisher Sciences, USA] antibody at room temperature for 40 minutes. Coverslips were counter-stained with DAPI and mounted on frosted microscope slides [Fisher Scientific, USA] using Vector shield mounting media [Vector Laboratories, Burlingane, USA]. DSB foci were quantified as described below.

2.4.3: Detection of NHEJ and HR DSB Repair Mechanisms

Homologous Recombination (HR) and Non-Homologous End Joining (NHEJ) are the two main DSB repair mechanisms. Rad51 and 53BP1 proteins are key factors involved in HR and NHEJ, respectively. They form foci that can be detected and used as markers of the corresponding DSB repair pathways. Therefore, to detect and measure HR and NHEJ, cells were stained with 53BP1 [Novus Biologicals, Centennial, USA] and Rad51[Abcam, USA] respectively. NHEJ/HR foci were quantified as described below. Labelling with DSB markers and DNA repair foci was carried out as follows: cells were co-stained with [γH2AX + Rad51] and [pATM + 53BP1] antibody pairs mixed in a single staining solution.

2.4.4: Assessment of NHEJ/HR DSB repair rates

HR and NHEJ are two mutually exclusive repair processes and can thus be distinctly assessed. The difference between the repair rates of both mechanisms was determined by quantifying the number of foci that got repaired within 1-6h after exposure to irradiation (repair fast component) and within

6 - 24h post-irradiation (repair slow component). Repair slopes were then measured and used as repair rates.

2.4.5: Microscopy imaging

Stained cells were visualized under a fluorescent confocal microscope. Nuclei stained with 1mg/ml DAPI (working concentration of 0.025ug/ml) were seen in the UV/blue channel, γH2AX and pATM foci were observed under the green channel and Rad51 and 53BP1 under the red channel. (Fig. 6). To create multichannel images, filters for each fluorophore: UV/blue, green and red, were set according to their wavelengths: 405, 488 and 594nm respectively. Images were taken at magnification 63X. Best signal configuration was selected, and a few modifications were made to separate overlapping fluorescence signals. Using the Z stack module, the first and the last plains were set to an optimal focus to capture every detail of the image and between 4-7 slices were taken at intervals of 1-2μm.

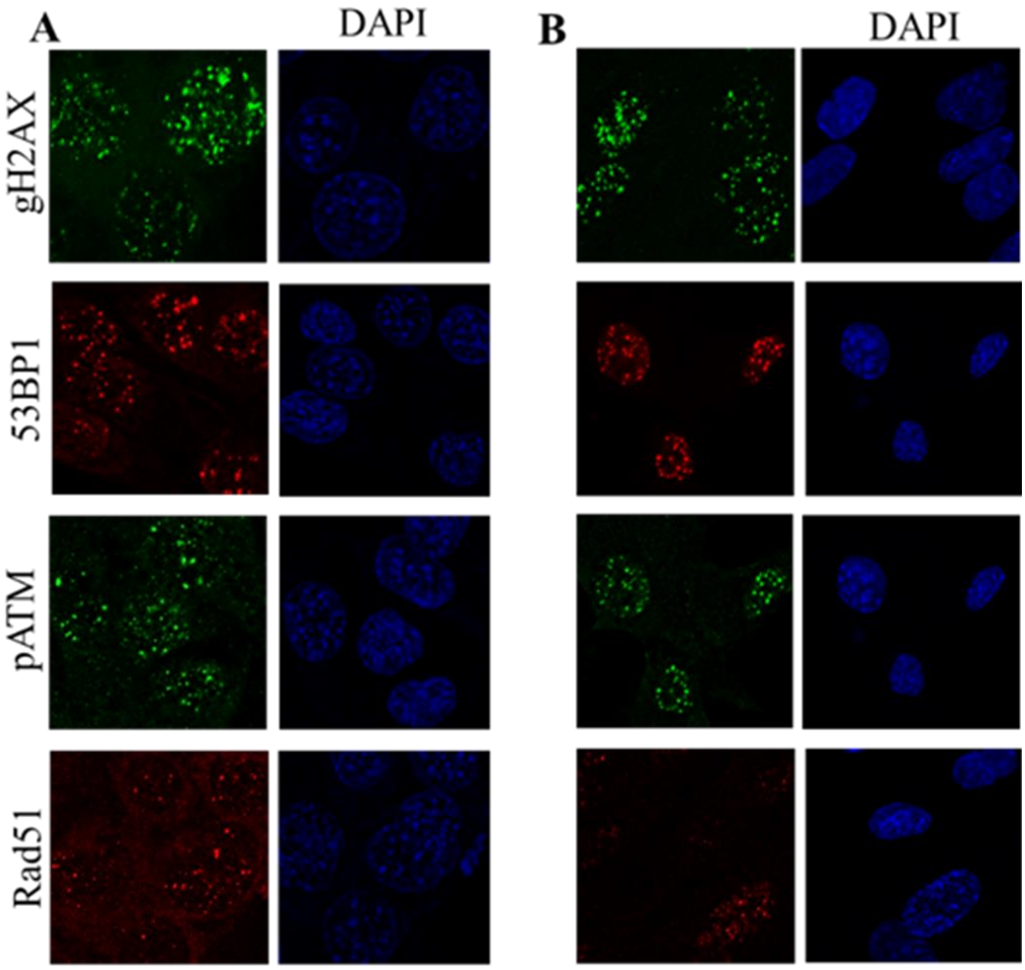
A
DAPI
B
DAPI
gH2AX
53BP1
pATM
Rad51

Fig. 6: Immunostaining analysis of DNA DSB sensors, pATM and γH2AX , as well as HR and NHEJ markers, Rad51 and 53BP1, respectively. Representatve images of γH2AX, 53BP1, pATM and Rad51 foci in C2C12 (A) and HSKM (B) at 1h following exposure to high dose 2Gy are shown. Blue staining represents nuclei counter-stained with DAPI.

2.5: Scoring of DSB/NHEJ/HR foci

Foci counter software (focicounter.sourceforge.net) was used to score foci. Parameters on the software were optimized for best correspondence to manual detection of foci by human expert eye. Median square side was set at 1, enhance parameter between 1 and 1.15, crown and rim radius at 1 and 3 respectively and brightness difference at 20. An average of 100 cells were scored from each treatment group.

2.6: Differentiation into the myogenic lineage

2.6.1: Mouse myotube Immunofluorescence staining

Immunofluorescence analysis of Myosin Heavy Chain (MyH3) protein was performed at time points: 0, 4, 8 and 12 weeks following initial irradiation. Myoblasts were grown on glass coverslips and assessed 24h post seeding under a light microscope to check viability and confluence of cells. Cells were monitored daily and allowed to reach confluence prior the initiation of differentiation. Afterwards, differentiation media was added (DMEM media, 1% Pen Strep, 2% FBS, 0.1% of 5mg/ml Transferrin [Sigma-Aldrich, USA] and 0.1 % of 5mg/ml Insulin [Sigma-Aldrich, USA]) for 3-5 consecutive days. Media was aspirated and the cells were washed with DPBS. Next, the cells were fixed with 1% of 37% w/w formaldehyde solution [Fisher Scientific, Fair Lawn, NJ, USA] in PBS for 30 minutes at room temperature. The samples were then washed thrice in PBS and stored in PBS at 4oC until IFM staining. To continue with staining process, myotubes were permeabilized with 0.2% Triton-X-100 [Sigma, St Louis, MO, USA] for 15 minutes and incubated in blocking buffer (10% FBS in 1X PBS, 0.02% Triton-X-100). Afterwards, samples were stained with 200ul of MyH3 at a dilution of 1:50 for 1hr at RT or 16h at 4oC and kept in a humid chamber over the period

of incubation. Following three washes in 1X PBS, cells were labelled with secondary antibody: Alexa Fluor 488 at 1:350 dilution for 30mins and with DAPI (1ug/ml) for 15 minutes. 100ul of Vectashield Mounting media was used to mount coverslips on Microscope slides which were subsequently stored at 4oC or visualized immediately under an EVOS M5000 Imaging System.

2.6.2: Human Myotube IFM staining

Immunofluorescence analysis of MyH3 protein [Santa Cruz Biotechnology, California, USA] were performed at 0 and 2 weeks following primary exposure to radiation. Myoblasts were grown on GG-20 collagen coated glass coverslips [Neuvitro Corporation, Vancouver, USA] because of the sensitivity of human cells and previous failure in growing them on plain glass coverslips. Differentiation and staining steps were precisely followed as with mouse samples.

2.6.3: Fusion Index Analysis

An average of 10 images were taken to represent each treatment group under magnification 20x. Cells were scored based on the degree of fusion. ImageJ software was used to quantify the fluorescent microscopy data. Nuclei in fibres were counted and myogenic capacity calculated using fusion index equation (Fusion Index = N_{fused}/N_{total} x 100%).

2.7: DNA repair gene expression measurement

To determine changes in gene expression, quantitative Reverse Transcriptase – Polymerase Chain Reaction (RT-qPCR) was used. Cells were seeded on 60 x 15mm plates and allowed to reach 70-80% confluence, irradiated and harvested at time points: 0, 6h, 24h, 1 week, 4 weeks, 8 weeks and 12 weeks following exposure and kept at -80^{o}C until RNA extraction using RT2 first strand kit and further analysis. Nanodrop spectrophotometer was used to determine the concentration of the purified total RNA, and RNA Stdsens Reagents and chip experion kit [BioRad, USA] to measure

the integrity. For reverse transcription of the purified RNA into cDNA, RT^2 First Strand kits (Qiagen, Hilden, Germany) was implemented as per manufacturer's instructions. In total, 500ng of RNA was used for each RT reaction. Amplification and quantification of the template cDNA was achieved through the use of 2X SYBR Green qPCR Master Mix [Bimake Biotech, Houston, USA]. Real-Time System, CFX 384 PCR machine [BioRad, USA] was set to optimal for the amplification of cDNA samples and to collect their respective Cycle threshold (Ct) values. Each cDNA was amplified in duplicates, the average of which was used to assess gene expression using RT^2 Profiler PCR arrays, Mouse DNA repair [Qiagen Sciences, Maryland, USA]. Data were analyzed using the Qiagen web-software such that the Cts of the genes were first normalized with housekeeping genes: ACTB, B2M, GAPDH, HS90AB1 and subsequently expressed as fold changes.

2.8: Measurement of Genomic Instability

Changes in the genome were visually determined using IFM assay. Cells were stained with DAPI and manually assessed for micronuclei and anaphase bridges which are markers of Genomic Instability. Images were taken under magnification 40X and an average of 2000 cells were examined in a cross-sectional order.

2.9: Assessment of Proliferation

Proliferation capacity of cells was measured using Incucyte Live Assay. This technique allows the imaging of live cells which were seeded as triplicates on 48-well plates and followed for up to 5 days. Growth rate curves were generated using Incucyte software confluency algorithm and exponential portions of the curves were used to calculate growth rates (slopes).

CHAPTER 3: RESULTS

3.1: LDR improves myogenic retention capacity in ageing myoblasts

The functional deficit of skeletal muscle cells is a feature of aging that has been confirmed in various studies [148]. In an in vitro study conducted by Soji Sebastian, a researcher at the Canadian Nuclear Laboratories, mouse skeletal MuSC were shown to deteriorate in function as they aged but exposure to 10 and 100 mGy doses of gamma radiation slowed down the deterioration process [unpublished, manuscript in preparation]. Similar experiments were repeated in this study using C2C12 mouse muscle myoblasts, and HSKM primary human myoblasts, as our study models.

3.1.1 Effects of LDR on myogenic capacity in C2C12

In aged animals, the size and the number of myofibers decrease, resulting in lower muscle mass and cross-sectional area. Given the reports on the benefits of LDR in stem cells particularly, the stimulation of differentiation [14, 20], mouse skeletal muscle myoblasts (C2C12) were investigated for the effects of LDR on their myogenic capacity. C2C12 cells were forced into quiescence by 48h incubation in a cellulose containing media - to mimic the state of such cells in human patients in vivo upon LDR medical procedures. Immediately upon the termination of quiescence conditions – removal from the methylcellulose gel and the placement into growing media - cells in suspension were treated with acute doses of 0 (sham-irradiated), 10, 100 and 2000mGy. Irradiated cells were then quickly plated in petri dishes and maintained normally over a period of 12 weeks and their capacity to differentiate was measured at time points 0, 4, 8 and 12 weeks. As seen in Fig. 7, young unirradiated myoblasts displayed the highest rate of formation of myotubes. As the cells aged, differentiation capacity declined, and fusion index dropped significantly from 60% to 10% at week

12. However, cells exposed to low doses 10 and 100mGy displayed a higher myogenic capacity compared to age-matched control. Interestingly, high dose irradiation with 2000mGy did not affect the aging related decline of the myogenic differentiation.

The results of this study demonstrated a beneficial effect of LDR on the retention of myogenic capacity in aged myoblasts.

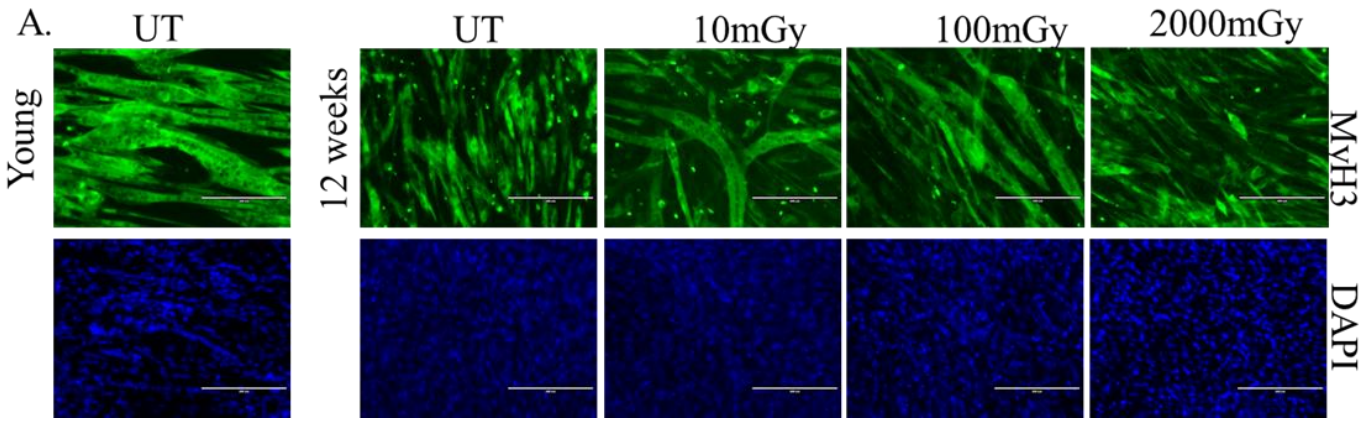
A.
UT
UT
10mGy
100mGy
2000mGy
Young
12 weeks
MyH3
DAPI

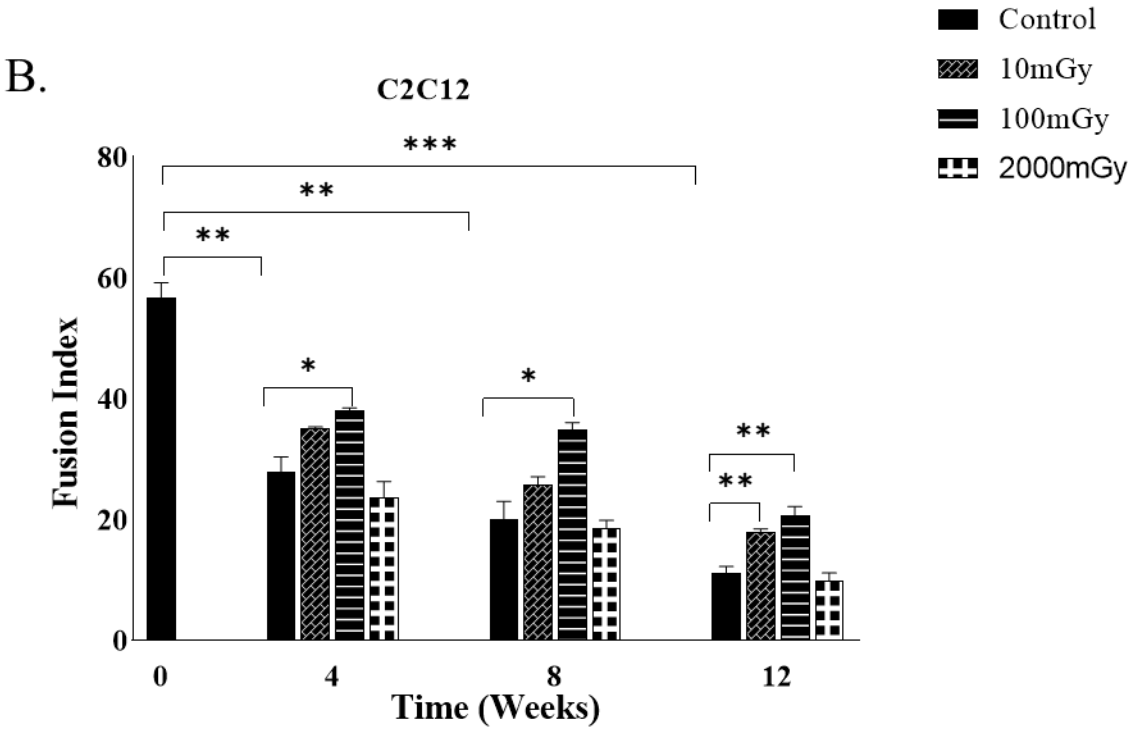
B.
C2C12
Control
10mGy
100mGy
2000mGy
Fusion Index
Time (Weeks)
0
4
8
12
0
20
40
60
80
***
**
**
*
*
**
**

Fig. 7: Exposure of C2C12 myoblasts to LDR at early passages leads to improved retention of the myogenic capacity over the period of 12 weeks following irradiation. A: Microphotographs of myofibers formed by early (Young) or late passaged (12 weeks) myoblasts exposed to 10, 100 or 2000mGy, or left untreated (UT). Myofibers were labelled with anti-Myosin heavy chain 3 antibody (MyH3, green) and counterstained with DAPI (blue). B: Quantification of the fusion index in myofibers as a measure of myogenic capacity of C2C12 myoblasts at indicated time points following exposure to IR. Data represent means of three independent experiments. Error bars represent Standard Error. Comparisons were made using two-way ANOVA (Tukey's method). *, ** and *** mark statistical significance at $p<0.05$,<0.01 and <0.001, respectively

3.1.2 Effects of LDR on myogenic capacity in HSKM

Primary human skeletal muscle myoblasts (HSKM) can divide only a limited number of times in comparison with immortalized mouse C2C12 myoblasts line and are known to very rapidly lose their functional properties within a short period of time. Therefore, HSKM cannot be maintained in culture for much longer than 2 weeks. In this study, HSKM cells were assessed for their functional capacity over a period of 2 weeks. Similar to their mouse counterparts, HSKM were taken out of the methylcellulose gel (quiescent state) and immediately exposed to acute doses of 0, 10 and 100mGy. Following this exposure, myoblasts were assessed at time points: 0 and 2 weeks for their ability to differentiate and fuse to form fibres. The results showed that myogenic capacity in the young control was not as high as in the mouse cells, however, the cells also displayed significant reduction of myogenic capacity from 30% fusion index in the young myoblasts to 25% in the 2-weeks old samples (Fig. 8). Although, exposure to low doses of 10 and 100mGy produced a trend towards higher efficiency of myotube formation, the comparison with the age-matched unirradiated sample produced a non-significant difference with $p=0.055$ (two-way ANOVA). It is interesting whether the lack of notable improvement of the myogenic capacity in human primary myoblasts may be associated with the subtle deterioration of this capacity within the explored time period of 2 weeks and if a more notable difference could be obtained at longer times after LDR exposure. These results show that, whereas not beneficial, LDR at least does not have a detrimental effect on myotube formation in in vitro expanded human myoblasts.

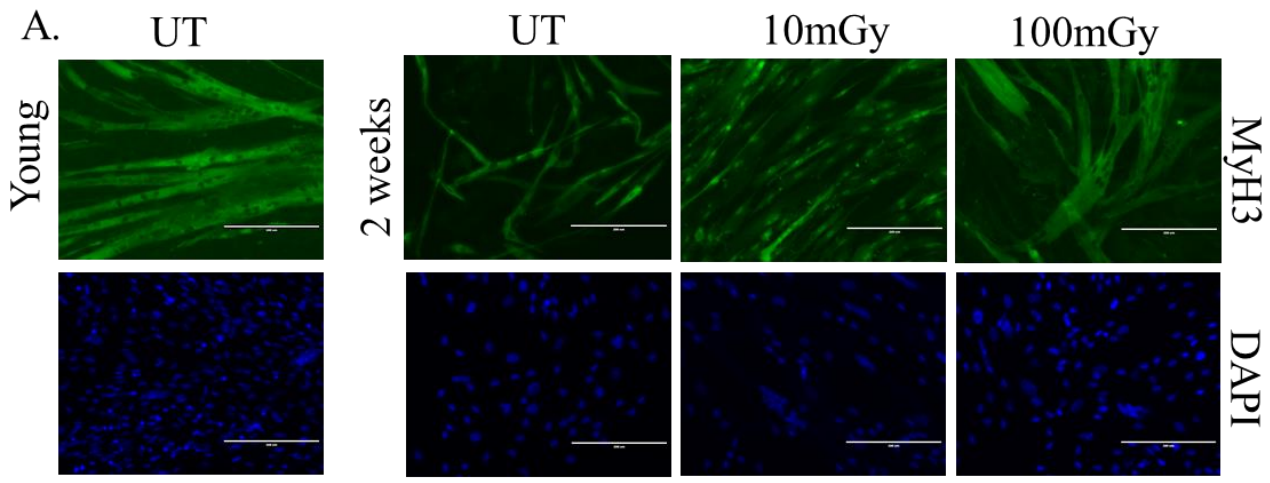
A.
UT
UT
10mGy
100mGy
Young
2 weeks
MyH3
DAPI

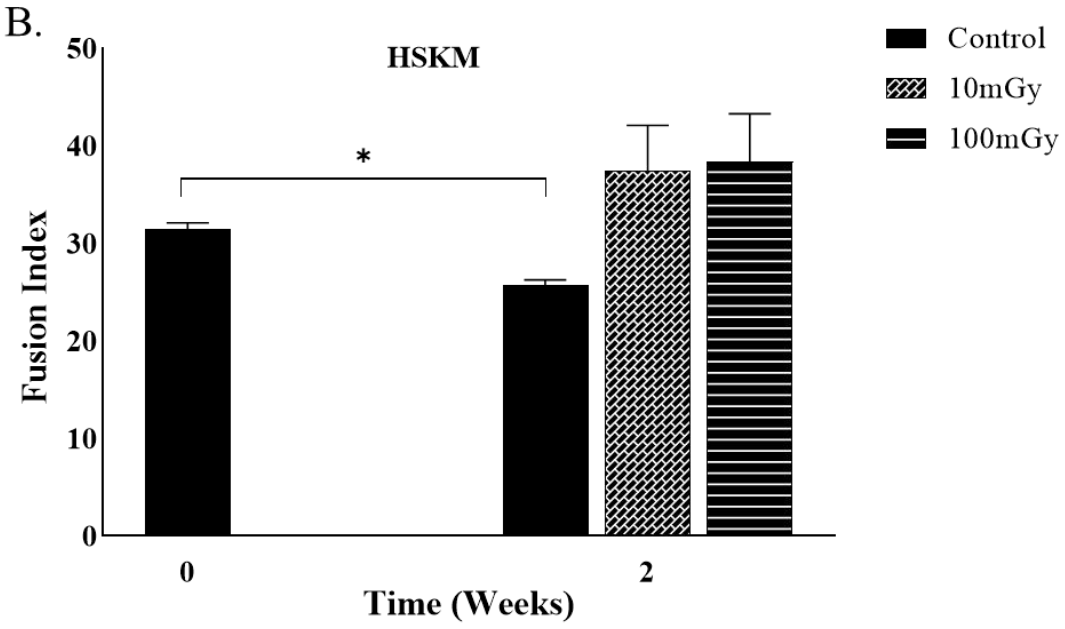
B.
HSKM
Control
10mGy
100mGy
Fusion Index
50
40
30
20
10
0
*
0
2
Time (Weeks)

Fig. 8: exposure of HSKM human primary myoblasts to LDR does not significantly affect the retention of the myogenic capacity over the period of 2 weeks following irradiation. A: Microphotographs of myofibers formed by early (Young) or late passage (2 weeks) myoblasts exposed to 10 or 100mGy or left untreated (UT). Myofibers were stained with anti-Myosin heavy chain 3 antibody (MyH3, green) and counterstained with DAPI (blue). B: Quantification of the fusion index in differentiated primary human myoblasts with or without irradiation. Data represent means of three independent experiments. Error bars represent Standard Error. Comparisons were made using one-way ANOVA. * marks statistical significance at $p<0.05$.

3.2: LDR suppresses GI

Another phenotype generally known to be associated with aging is genomic instability. Having confirmed the beneficial effects LDR produced with respect to the functional capacity of aging mouse myoblasts, the genome was examined for gross chromosomal aberrations, such as anaphase bridges and micronuclei, known to be associated with GI. Anaphase bridges (AB) (Fig. 9a) and micronuclei (MN) (Fig. 9b) were counted and scored relative to the number of anaphase cells and DAPI stained nuclei respectively.

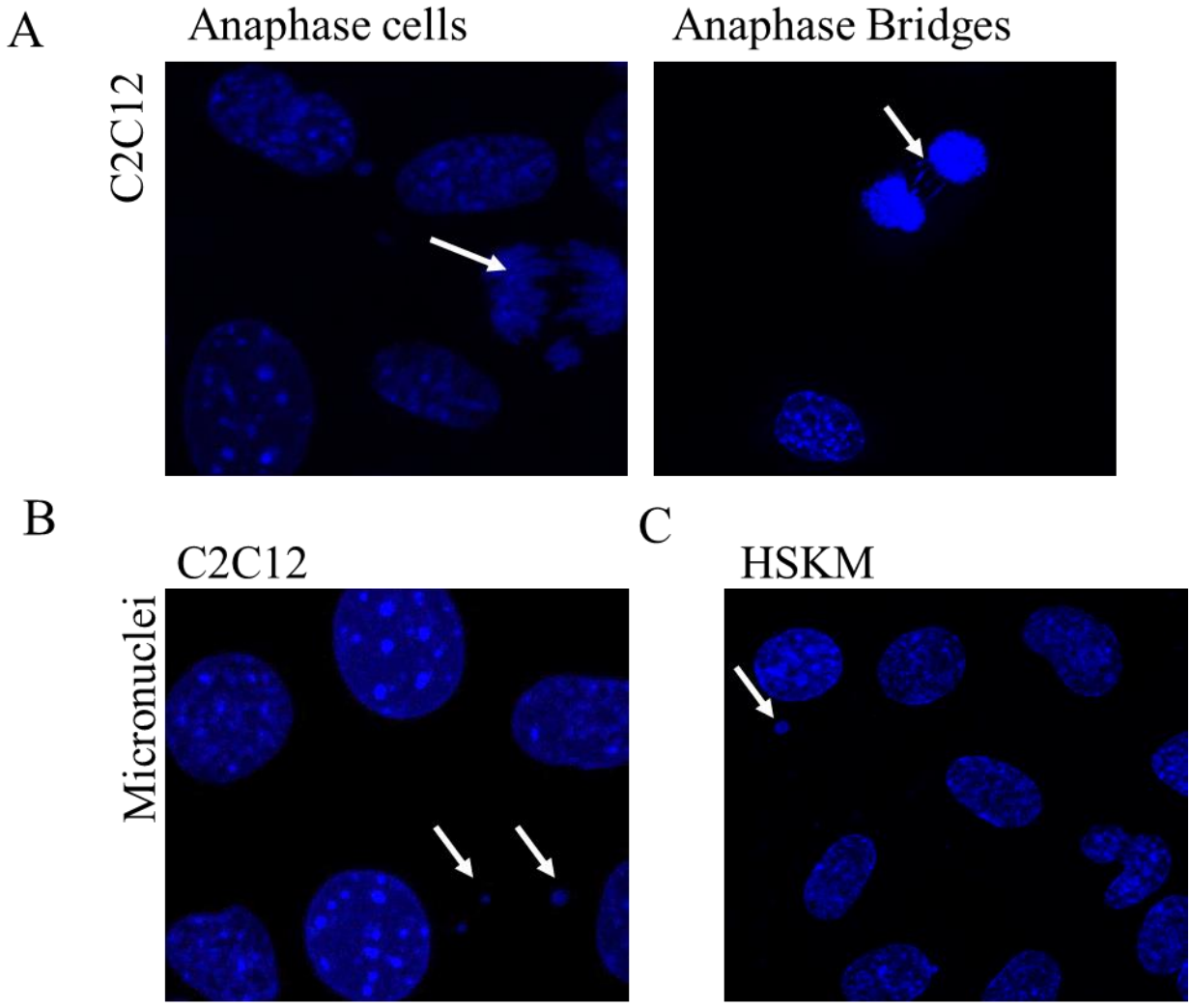
A
Anaphase cells
Anaphase Bridges
C2C12
B
C2C12
Micronuclei
C
HSKM

Fig. 9: Representative microscopy images of DAPI-stained cells showing A) normal anaphase cells (first panel) and anaphase bridges during cell division and B) micronuclei in C2C12 and C) HSKM.

3.2.1: Effects of LDR on GI in C2C12

The functional deficit of satellite cells as a feature of aging is a strong cell-intrinsic and irreversible component that could be partially mediated by GI [149]. GI in C2C12 was measured by quantifying the rates of AB and MN. Firstly, it was observed that unirradiated mouse myoblasts showed no consistent linear increase in AB with age, and cells at 12 weeks displayed the highest levels of AB (Fig. 10a). Moreover, compared to the age-matched control, there was a statistically significant reduction of AB in 100mGy exposed cells at 12 weeks. Secondly, the rate of AB in HDR-exposed cells was similar to that seen in unirradiated cells. Thirdly, LDR-exposed cells tended to display lower levels of AB compared to age-matched untreated control. Two-way ANOVA analysis indicated that LDR treatment resulted in a significant reduction of anaphase bridges ($p=0.03$), with the multiple comparison Fisher LSD method revealing that specifically 100mGy treated cells exhibited significantly lower levels of anaphase bridges vs. control.

Also, MN count was determined by examining 2000 cells in each treatment group. The results showed an age-dependent increase in the MN rates, yet the increase was not linear. LDR resulted in the reduction of the MN frequencies compared to age-matched controls (Fig. 10b). Cells exposed to HDR exhibited higher rates of micronuclei compared to untreated at week 12 (Fig. 10b).

Overall, the results from the AB and MN analysis suggests that LDR suppressed genomic instability in mouse myoblasts.

A

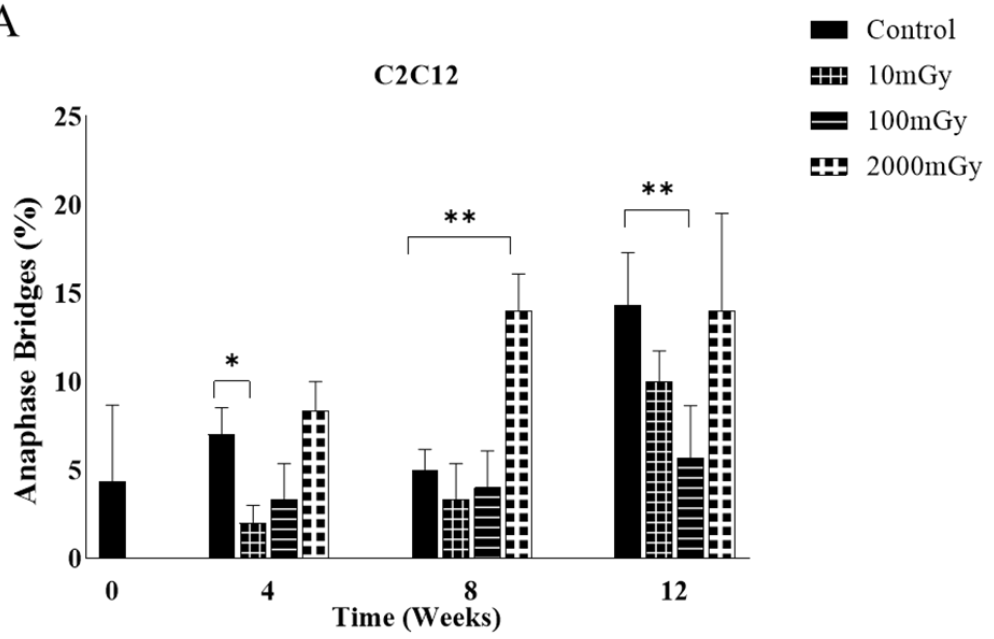
C2C12
Control
10mGy
100mGy
2000mGy
Anaphase Bridges (%)
25
20
15
10
5
0
*
**
**
0
4
8
12
Time (Weeks)

B

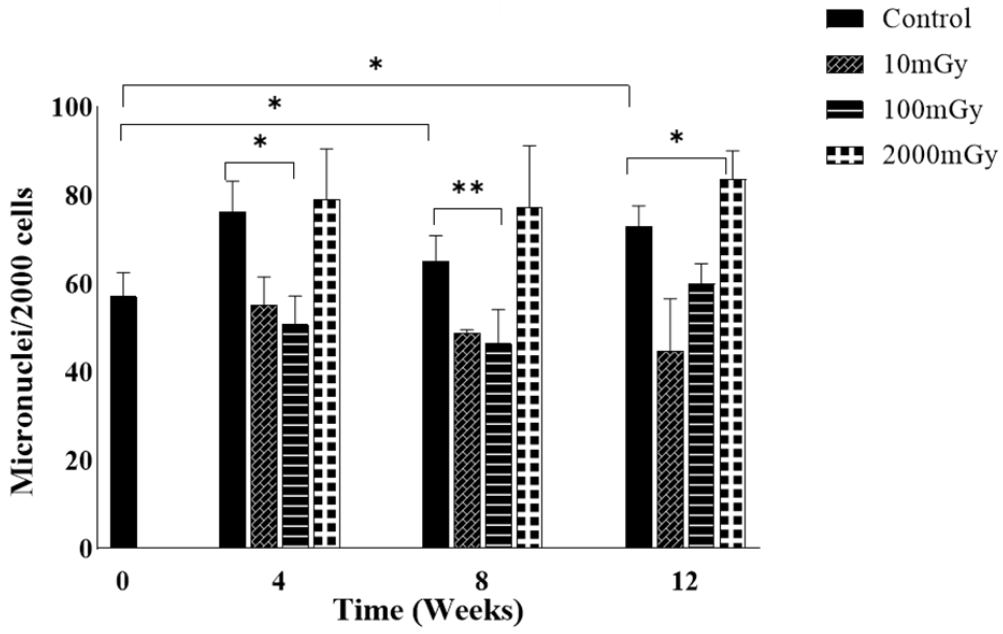
Control
10mGy
100mGy
2000mGy
Micronuclei/2000 cells
100
80
60
40
20
0
*
*
*
**
*
0
4
8
12
Time (Weeks)

Fig. 10: Exposure of C2C12 myoblasts to LDR at early passages suppresses genomic instability over the period of 12 weeks following irradiation. Quantification of anaphase bridges (A) or micronuclei (B) at indicated time points after exposure of early passage cells to 10, 100 or 2000mGy or in sham-exposed (UT) cells. Percentage of anaphase bridges relative to a total number of anaphase cells is shown in A) and the number of micronuclei per 2000 cells is shown in B). Comparisons were made using Two-way ANOVA (Tukey's method) and LSD Fisher method for AB and MN, respectively. * and ** mark statistical significance at $P<0.05$ and <0.01, respectively.

3.2.2 Effects of LDR on GI in HSKM

MN were used as the only marker for genomic instability detection in human myoblasts because of insufficient number of anaphase cells available for scoring anaphase bridges (Fig. 9c). Quantitation of MN revealed no changes in GI between aged LDR treated cells and untreated myoblasts. However, a significant difference was seen between the aged and young untreated cells, indicating that GI is a feature of the aging phenotype in these cells (Fig 11).

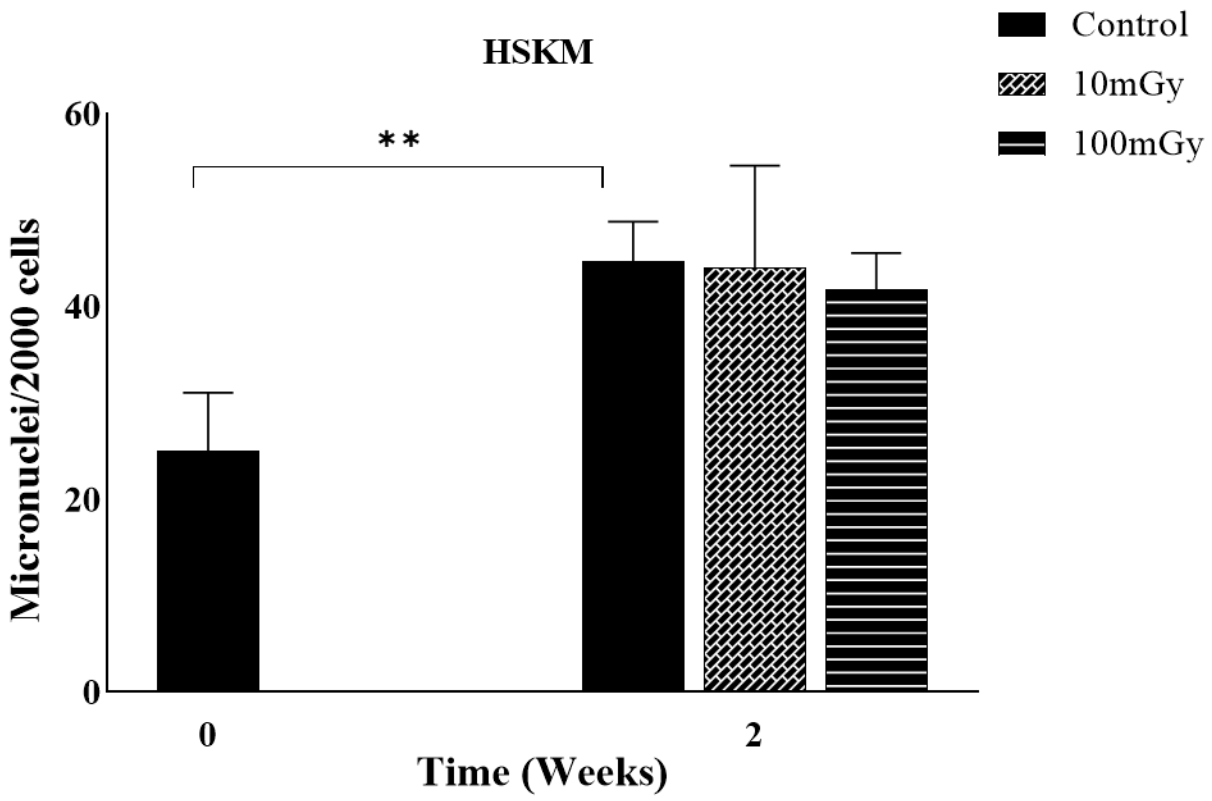
HSKM
Control
10mGy
100mGy
**
60
40
20
0
Micronuclei/2000 cells
0
2
Time (Weeks)

Fig. 11: Exposure of HSKM primary human myoblasts to LDR at early passages does not affect genomic instability over the period of 2 weeks following irradiation. Genomic instability was assessed by measuring the number of cells with micronuclei per 2000 total cells in cultures exposed to 10 or 100mGy or left untreated (UT) at early passage (t=0). Shown are means of three independent experiments. Error bars represent Standard Error. Comparisons were made using One-way ANOVA. ** marks the statistical significance at $p<0.01$.

3.2.3: *LDR does not affect endogenous DNA damage*

In addition to AB and MN formation, another manifestation of GI at the molecular level is the persistence of endogenous DNA damage [150]. In this study, GI was also evaluated by measuring the basal levels of microscopic foci formed by DNA damage response proteins pATM, γH2AX, 53BP1 and Rad51 at time points 0, 4, 8 and 12 weeks. pATM and 53BP1 displayed no significant difference between control and LDR-exposed cells at any of the time points (Fig. 12b and c). However, γH2AX foci showed a trend towards lower levels in LDR-treated myoblasts at week 12 (Fig. 12a). A study showed that differences in the levels of γH2AX foci compared with pATM foci did exist, suggesting that H2AX phosphorylation status can be independent of activated ATM and more persistent than pATM [151]. Also, at week 8, LDR treated myoblasts displayed lesser number of Rad51 foci compared to the control (Fig 12d).

Since these measurements were done many weeks after the initial LDR exposure, it is feasible to suggest that the foci measured represented in this case the endogenous levels of DSB, not the damage induced by the LDR itself. The results showed variable effects of LDR on endogenous damage in the DNA, most likely DSB, suggesting that the LDR does not significantly affect the formation and processing of endogenous DNA breaks in aging myoblasts.

In the primary human cells model, although non-significant, basal levels of γH2AX and Rad51 foci revealed slight changes with LDR. Aside this, measurements with the other proteins displayed no change with LDR exposure, neither with age, nor with IR (Fig. 13).

Overall, the results from the GI study showed the suppression of age-related GI in LDR exposed mouse myoblasts as determined by the quantitation of MN and AB. This effect was not seen in human primary myoblasts.

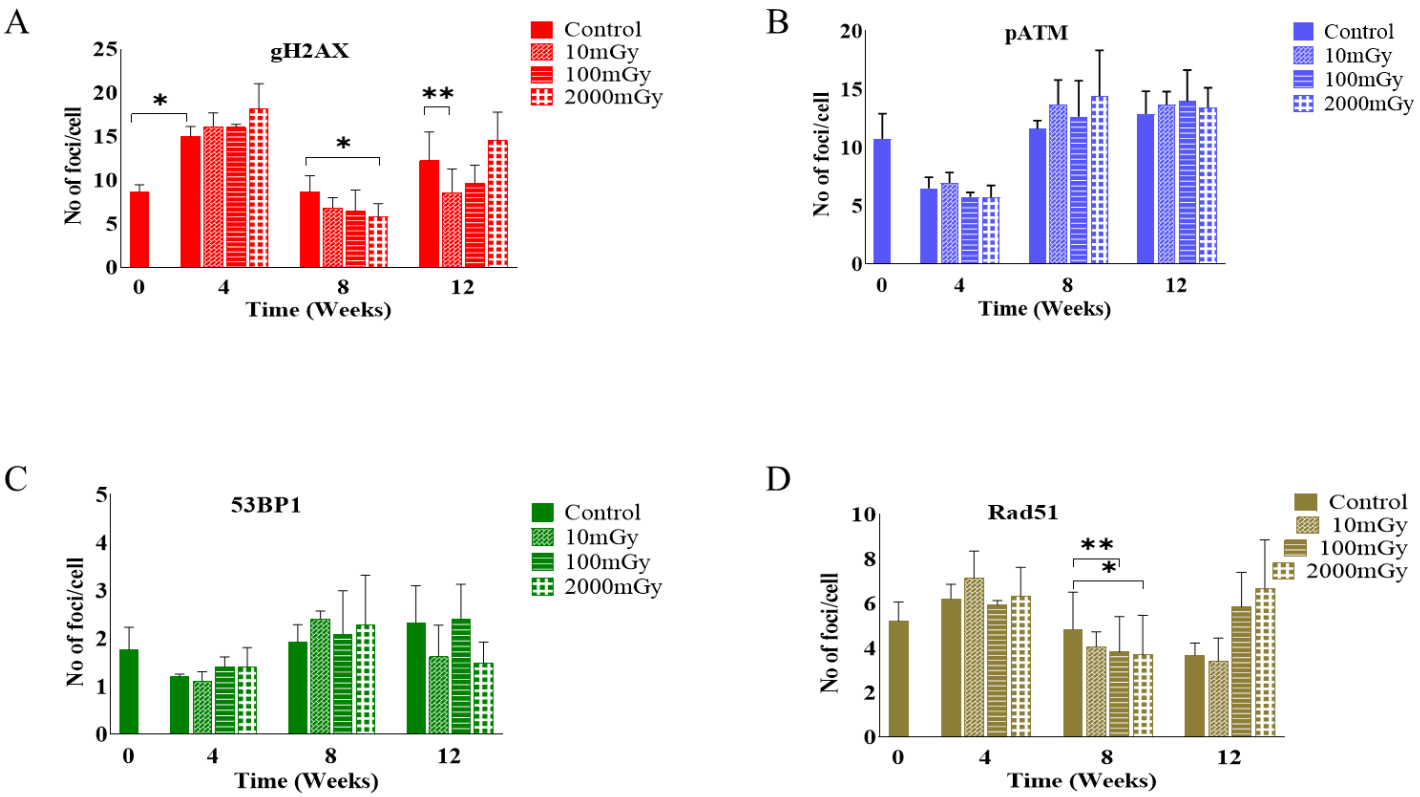
A
gH2AX
No of foci/cell
Time (Weeks)
Control
10mGy
100mGy
2000mGy
B
pATM
No of foci/cell
Time (Weeks)
Control
10mGy
100mGy
2000mGy
C
53BP1
No of foci/cell
Time (Weeks)
Control
10mGy
100mGy
2000mGy
D
Rad51
No of foci/cell
Time (Weeks)
Control
10mGy
100mGy
2000mGy

Fig. 12: Exposure of C2C12 myoblasts to LDR at early passages does not affect the basal rates of DSB and/or DSB signalling over the period of 12 weeks following irradiation. Cells were irradiated at t=0 and DSB repair foci of γH2AX (A; red), pATM (B; blue), 53BP1 (C; green) and Rad51 (D; brown) proteins were detected using immuno-fluorescence microscopy at time points 0, 4, 8 and 12 weeks post-irradiation. Shown are means of three independent biological replicates. Error bars represent Standard Error. Comparisons were done using Student's paired one-tailed t-test. * and ** mark statistical significance at $p<0.05$ and <0.01 respectively.

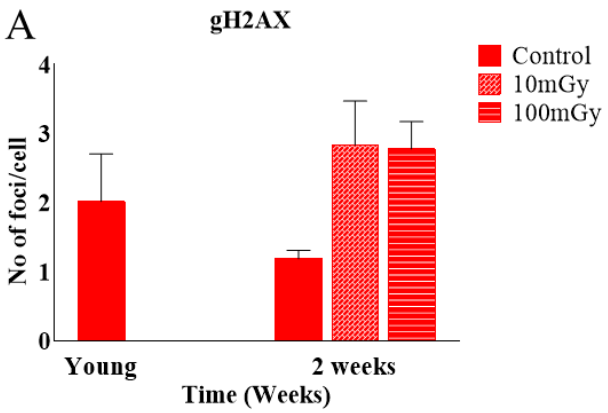
A
gH2AX
Control
10mGy
100mGy
No of foci/cell
0
1
2
3
4
Young
2 weeks
Time (Weeks)

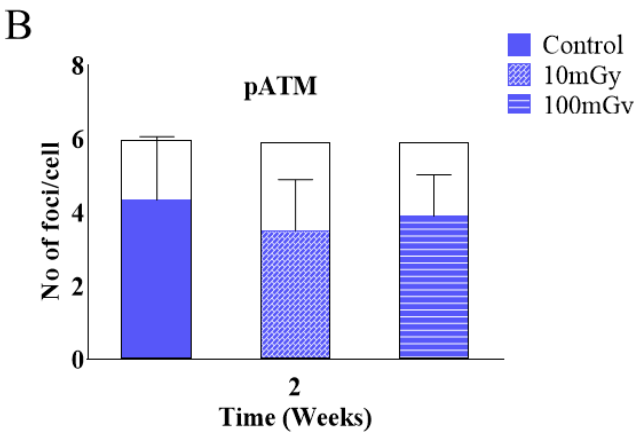
B
pATM
Control
10mGy
100mGv
No of foci/cell
0
2
4
6
8
2
Time (Weeks)

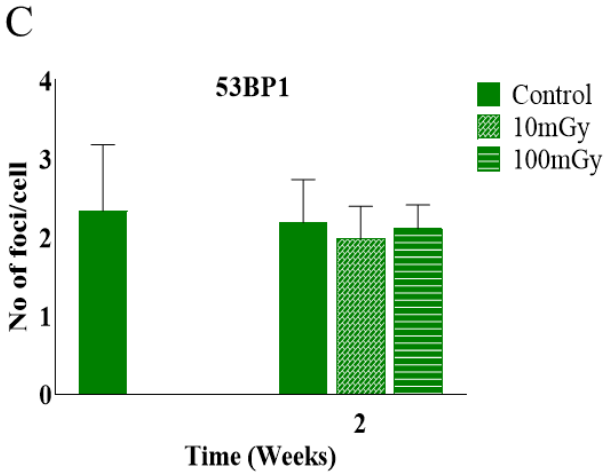
C
53BP1
Control
10mGy
100mGy
No of foci/cell
0
1
2
3
4
2
Time (Weeks)

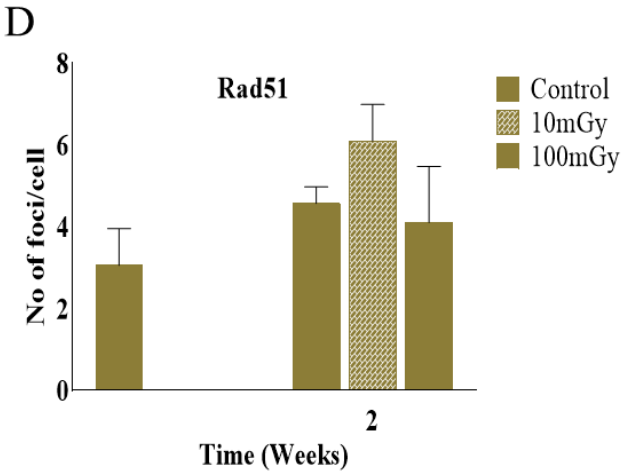
D
Rad51
Control
10mGy
100mGy
No of foci/cell
0
2
4
6
8
2
Time (Weeks)

Fig. 13: Exposure of HSKM primary human myoblasts to LDR at early passages does not affect the basal rates of DSB and/or DSB signalling over the period of 2 weeks following irradiation. Cells were irradiated at t=0 and foci of γH2AX (A; red), pATM (B; blue), 53BP1 (C; green) and Rad51 (D; brown) proteins were detected using immuno-fluorescence microscopy at time points 0 and 2 weeks. Shown are means of three independent biological replicates. Error bars represent Standard Error. No significant changes were found using Student's paired one-tailed t-test.

3.3: DNA repair was affected by exposure to LDR

The classic mutator hypothesis postulates that a loss of DNA repair capacity leads to GI which in turn increases mutation rates at other genomic loci, leading to cellular transformation [152]. DNA repair capacity can diminish via several mechanisms and can broadly be evaluated by examining gene expression levels. To determine whether the increased GI in the age-long unirradiated population was driven by the compromised expression of DNA repair genes, gene expression analysis of 84 genes was performed. The panel of genes is presented in Table 1 (Qiagen RT2 PCR Mouse DNA Repair profiler array) and includes major genes involved in various DNA repair pathways. RNA was extracted from samples exposed to 0mGy, 10mGy, 100mGy and 2000mGy, purified and quantified, transcribed to cDNA templates and amplified in duplicates using qPCR. Gene expression data was normalized to 5 housekeeping genes and fold-changes were calculated using the delta-delta Ct method. This analysis was only carried out in C2C12 cells at time points 0, 6 & 24h and 1, 4, 8 and 12 weeks. The following observations were drawn from the analysis.

Age-related modulation of genes was observed at 1, 8 and 12 weeks in the unirradiated samples. The highest level of downregulation of repair genes was observed in the HDR samples after 24h. On the other hand, LDR exposure induced a broad activation of repair pathways as the treated cells displayed an upregulation of 18 repair genes at 4 weeks following IR exposure: five Base Excision Repair (BER) genes, two Nucleotide Excision Repair (NER) genes, four Homologous Recombination (HR), two Non-Homologous End Joining (NHEJ), three Mismatch Repair (MR) (Fig. 14).

However, most of the upregulation had disappeared by the last week of analysis (week 12) and only 4 genes: Msh4, Rpa1, Top3a and Xrcc5 were upregulated in cells exposed to10mGy. 100 and 2000mGy displayed no significant changes compared to control at week 12 (Table 2).

Msh4 is a mismatch protein involved in the formation of crossovers during meiosis. This protein forms a heterodimer with Msh5, which binds uniquely to a double Holliday Junction (dHJ) and stabilizes the interaction between parental chromosomes during meiosis DSB repair [153]. Rpa1 is also required for the recruitment of DSB repair factors: Rad51 and Rad52 to chromatin in response to DNA damage [154]. Likewise, Top3a forms a part of the complex that processes dHJs that arise as a result of HR-mediated repair of DSB during DNA synthesis [155]. On the other hand, Xrcc5 is a gene that encodes for Ku80, a protein known for its involvement in the repair of DSB by NHEJ [156].

It can be broadly concluded from this data that LDR exposure of young mouse myoblast cultures resulted in global activation of the expression of genes involved in various DNA repair pathways. There were more genes activated that belonged to HR than to NHEJ; however, activation of multiple BER genes was also evident. Although, a decline in such response was observed at 12 weeks post-LDR exposure, four genes involved in DSB repair were still overexpressed. The elevated levels of mRNA of DNA repair genes at such prolonged periods after LDR exposure may render cells more resistant to both exogenous and endogenous DNA lesions resulting in enhanced genomic integrity and functional fitness.

Table 1: List of 84 genes involved in various DNA repair pathways that were analysed in this study using RT-qPCR arrays technology

BER	**NER**	**HR**	**NHEJ**	**MR**	MGMT	
APEX1	ATXN3	ATM	LIG4	EXO1	SLK	
APEX2	CCNH	ATR	PNKP	MLH1	ACTB	
ATXN3	CCNO	BRCA1	POLL	MLH3	B2M	
CCNH	CDK7	BRCA2	PRKDC	MSH2	GAPDH	
FEN1	DDB1	BRIP1	XRCC4	MSH3	HSP90AB1	
LIG1	DDB2	MRE11A	XRCC5	MSH4	MGDC	
LIG3	ERCC1	RAD18	XRCC6	MSH5	RTC	
MPG	ERCC2	RAD50	XRCC6BP1	MSH6	RTC	
MUTYH	ERCC3	RAD51		PMS1	RTC	
NEIL1	ERCC4	RAD51C		PMS2	PPC	
NEIL2	ERCC5	RAD51L1		RFC1	PPC	
NEIL3	ERCC6	RAD51L3			PPC	
NTHL1	ERCC8	RAD52				
OGG1	MMS19	RAD54L				
PARP1	POLD3	RPA1				
PARP2	RAD23A	RPA3				
PARP3	RAD23B	TOP3A				
POLB	XAB2	TOP3B				
SMUG1	XPA	XRCC2				
TDG	XPC	XRCC3				
TREX1		DMC1				
UNG						
XRCC1						

HOUSEKEEPING GENES; GENOMIC DNA CONTROL; REVERSE TRANSCRIPTASE CONTROL; POSITIVE PCR CONTROLS

BER: Base Excision Repair; **NER**: Nucleotide Excision Repair; **HR**: Homologous Repair; **MR**: Mismatch repair

Table 2: Gene expression changes with aging; Downregulated genes highlighted pink and upregulated in green

CONTROL (Aging)		Gene Name	Fold Regulation	Fold value
1 week	UT	Apex1	-25.04	0.023739
		Apex2	-70.32	0.043483
		Atm	-81.63	0.042209
		Atxn3	-19.93	0.053086
		Brip1	-45.08	0.024612
		Ccno	-129.94	0.055728
		Ddb1	-24.65	0.003892
8 weeks	UT	Ccno	-77.83	0.02
		Ddb1	-7.97	0.01
12 weeks	UT	Apex1	-23.6	0.04
		Apex2	-73.31	0.04
		Atm	-194.74	0.04
		Brip1	-139.43	0.03
		Ccno	-754.18	0.02
		Ddb1	-43.44	0.00

Table 3: Gene expression changes with IR; Downregulated genes highlighted pink and upregulated in green

IR		Gene Name	Fold Regulation	Fold value
10mGy	24h	Rad51l3	-4.62	0.043638
	4 weeks	Atxn3	4.29	0.00
		Ccno	94.59	0.03
		Exo1	5.25	0.00
		Mpg	4.98	0.00
		Msh4	4.88	0.03
		Parp1	6.38	0.00
		Pnkp	4.33	0.00
		PPC	5.9	0.02
		Rad51	4.5	0.00
		Rad51c	4.07	0.00
		Rad52	4.55	0.00
		RTC	4.04	0.00
		Xrcc1	5.86	0.00
		Xrcc3	4.81	0.00
		Xrcc6bp1	4.27	0.04
	12 weeks	Msh4	4.25	0.00
		Rpa1	4.08	0.00
		Top3a	4.59	0.00
		Xrcc5	4.09	0.00

100mGy	24h	Trex1	-4.74	0.003027
	4 weeks	Exo1	4.54	0.00
		Msh5	5.05	0.04
		Neil2	5.23	0.02
		Parp1	4.39	0.01
		PPC	5.99	0.02
		Xpa	10.24	0.05
		Xrcc1	4.59	0.00
		Xrcc6bp1	4.01	0.01
2000mGy	24h	Atm	-9.06	0.05295
		Brca1	-7.3	0.001968
		Ercc3	-7.71	0.000656
		Ercc6	-4.41	0.001129
		Errc8	-4.37	0.026085
		Exo1	-4.05	0.013492
		Lig4	-4.21	0.008752
		Mlh3	-5.88	0.012075
		Pnkp	-5.27	0.006955
		Rad51l1	-8.32	0.016513
		Rad51l3	-8.75	0.040783
		Top3a	-5.33	0.006332

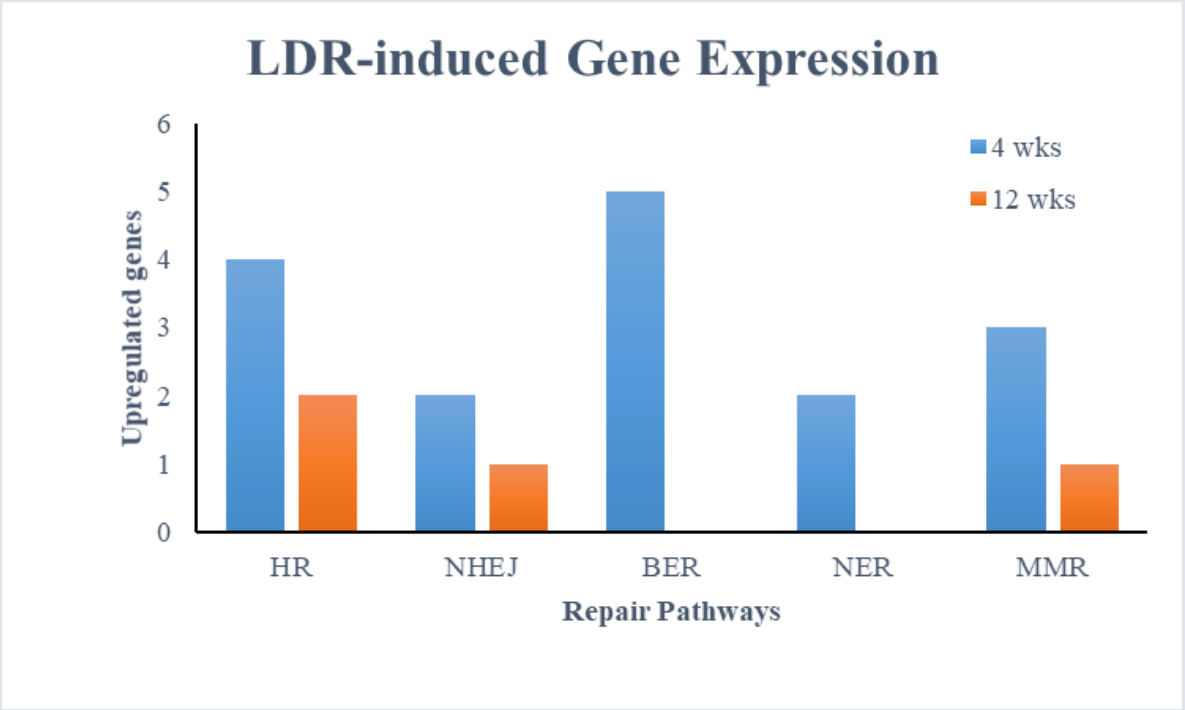

Fig. 14. Exposure of C2C12 myoblasts to LDR at early passages leads to more robust upregulation of HR vs NHEJ genes over the period of 12 weeks following irradiation. At t=0, cells were irradiated, with 0, 10 or 100 mGy and the expression of 84 DNA repair genes was measured by RT-qPCR. Number of significantly upregulated genes within each of the 5 DNA repair pathways was quantified and pooled for 10 and 100mGy using the online Qiagen data analysis portal. These number are shown on the plot. Predominant activation of HR vs NHEJ genes is seen for both 4- and 12-week time points. Upregulation of BER and NER at 4 weeks is also notable, however this was not observed at 12 weeks. **BER**: Base Excision Repair; **NER**: Nucleotide Excision Repair; **HR**: Homologous Repair; **MMR**: Mismatch repair

3.4: Overall repair of DSB did not change with LDR

3.4.1 Effects of LDR on DSB repair

Although DSB cannot be easily measured directly, several assays that provide a secondary marker of the extent of DSB damage can be used to visualize and quantify DSB and specific signalling pathways of DNA damage response (DDR). One of the earliest and universal events during DDR is the phosphorylation, by the kinases ATM, ATR and DNK-PKcs, of the histone isoform H2AX on serine residue 139 (P-S139) to form γH2AX [157]. γH2AX forms foci each consisting of up to a few thousand γH2AX molecules around a DSB. Therefore, γH2AX foci have been widely used to monitor DSB and their repair *in vitro* and *ex vivo* [158-159].

Since it was found that LDR is capable of modulating gross chromosomal damage characteristic of a GI phenotype and having links to DSB, it was interesting to examine whether LDR may also affect the functional capacity of a DSB repair machinery in exposed myoblasts over prolonged periods of

time after the LDR treatment. Of all the types of damage the DNA is liable to, DSB are among the most deleterious lesions [30]. DSB have the potential of increasing genomic instability if not repaired or if repair is improperly done. DSB triggers DNA damage response events which coordinate DNA repair. However, whether the accumulation of DNA damage with age is a result of decreased repair capacity, remains to be determined [4]. To determine whether the suppression of GI and the enhancement of function observed in the LDR-exposed myoblasts was associated with the overall repair of DSB, the induction of IRIF foci and their removal, was monitored.

3.4.2: Assessment of DSB repair capacity using γH2AX *and pATM foci in C2C12*

To assess repair capacity of DNA DSB, the following analyses were performed:

i. Assessment of DNA DSB induction and repair after a challenging 2Gy irradiation. γH2AX and pATM proteins are involved in the detection of DSB and can also be used to measure their repair by evaluating the appearance and disappearance of foci. To achieve this, myoblasts were exposed to primary doses of 0, 10, 100 and 2000mGy at t=0. Primed cells were then challenged to a secondary exposure of 2Gy at t=4, 8 and 12 weeks to induce DSB and to trigger DDR in aging myoblasts.

Formation and removal of IRIF was then studied by detecting and quantifying foci IRIF at 0, 1, 6 and 24h post-challenging 2Gy. DSB repair curves were then constructed and are presented in Fig. 15. It can be seen that both irradiation and age affected activation of the ATM protein at 1 and 6 hr, but not at 24h, post-challenge. Although non-significant, repair curves of LDR primed cells at weeks 4 and 8 reflected better induction of pATM (Fig. 15a). Asides this, there was no evident change in

DSB signalling. The induction of γH2AX foci varied with age producing no definite pattern and prior exposure to LDR did not affect DSB processing (Fig. 15b).

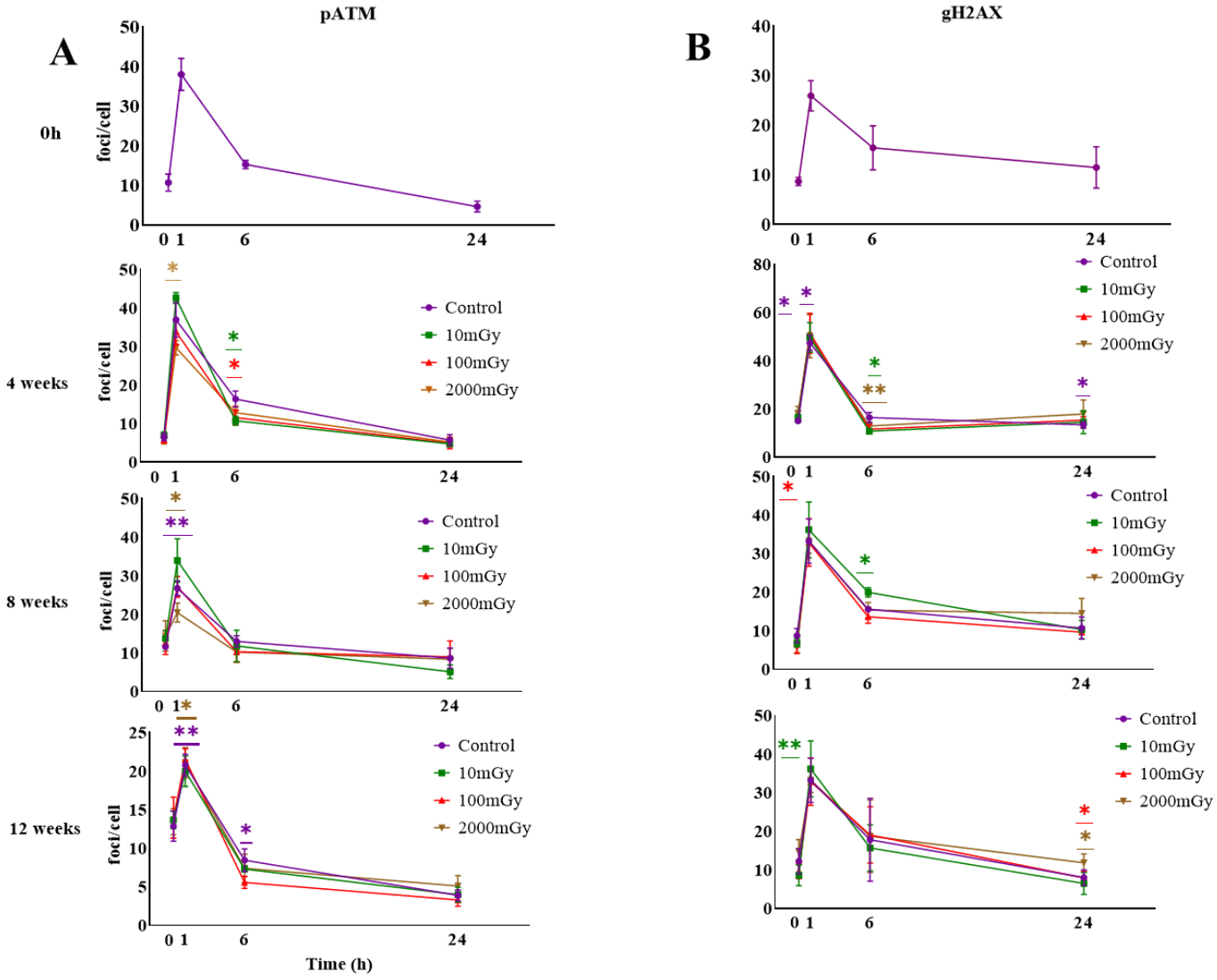
A
pATM
0h
4 weeks
8 weeks
12 weeks
foci/cell
Time (h)
Control
10mGy
100mGy
2000mGy
B
gH2AX

Fig. 15: Exposure of C2C12 myoblasts to LDR at early passages does not change cells ability to detect and repair exogenously induced DSB. Cells were exposed to priming gamma-irradiation at doses of 0 (Control), 10, 100 or 2000 mGy at t=0 and maintained by routine subculturing under normal growth conditions. At 0, 4, 8 and 12 weeks post-priming, cells were challenged with a high dose of 2000 mGy and the induced DSB were visualized as and scored as pATM (A) and γH2AX (B) foci using immuno-fluorescence microscopy at 0, 1, 6 and 24h post-challenge. Number of foci per cell was quantified and plotted resulting in foci repair curves. Although, statistical significance was observed between select exposure groups for some time points, overall, the differences are sporadic, indicating the lack of the effect of LDR on the cells ability to detect and repair gross DSB after a high-dose challenge. Exposure groups are color coded: sham irradiated, purple, 10mGy, green, 100mGy, red and 2000mGy, brown. Data are means of three independent experiments, with over 100 nuclei per data point scored in each biological replicate. Comparisons were done using Student's paired one-tailed t-test. Color coding of statistical significance signify comparisons between corresponding treatment groups and time-matched control. * and ** mark statistical significance at $p<0.05$ and <0.01, respectively.

ii. Fast and slow repair kinetics from γH2AX and pATM foci data. Foci induced at 1h represent robustness of the initial DNA DSB signalling, whereas at 6 and 24 h they indicate completion of DSB rejoining. Since the patterns were complex, the repair kinetics was split into fast and slow components (Fig. 16). The slope of repair between points 1 & 6h and 6 & 24h on the repair curves were calculated to determine the fast and slow repair rates respectively. The pATM foci graph (Fig. 16a) presented better fast repair with LDR at week 4 but was not sustained in older culture. This acceleration was accompanied by deceleration of the slow repair component. A similar trend was detected in γH2AX with both proteins displaying no changes in residual DSB levels in all groups.

These results revealed temporary modulation of the fast vs. slow repair rates by LDR, however, the effects did not last to 12 weeks post LDR exposure. In addition, a lack of the effect of LDR on residual foci at 24h is indicative of complete rejoining with or without priming with LDR.

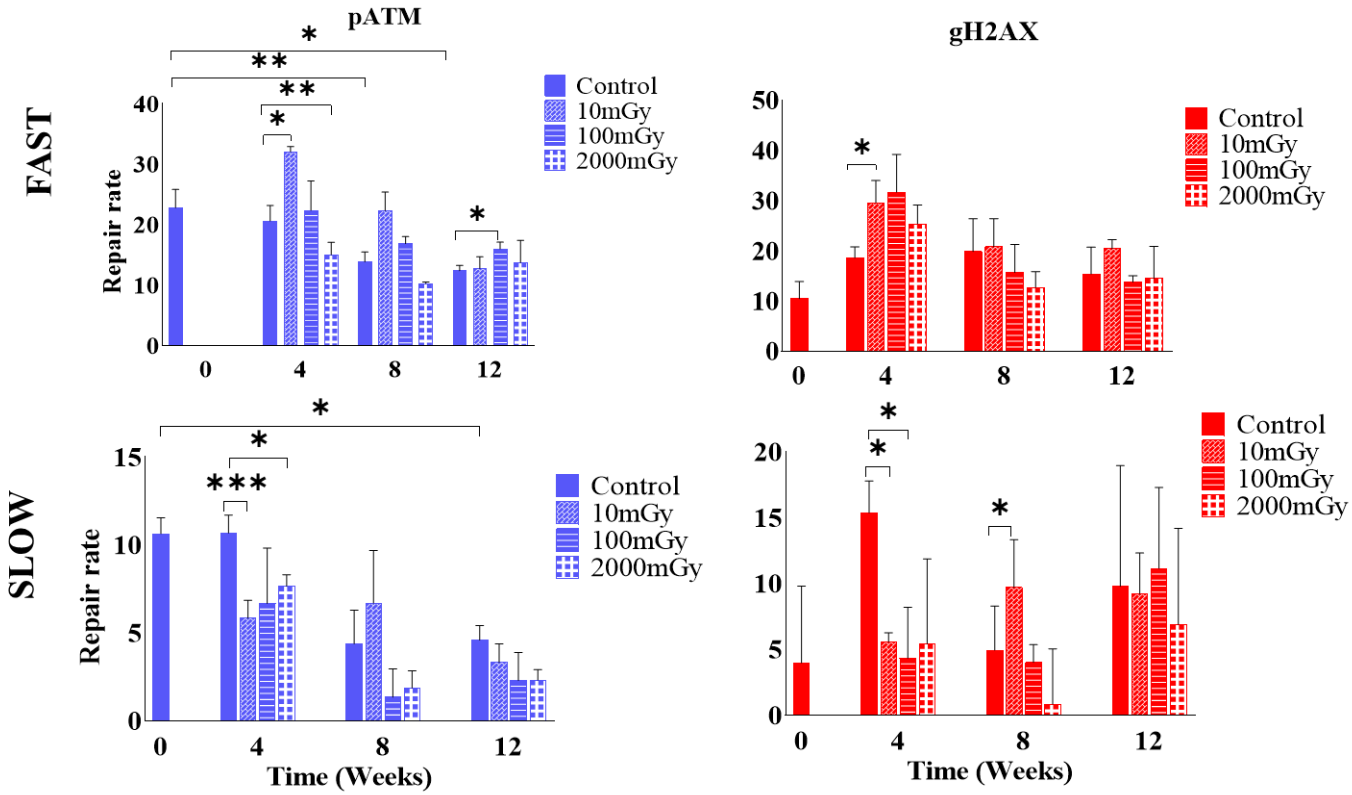
pATM
gH2AX
FAST
SLOW
Repair rate
Time (Weeks)
Control
10mGy
100mGy
2000mGy
0
4
8
12

Fig. 16: Exposure of C2C12 myoblasts to LDR at early passages differentially affects fast vs slow DSB repair components at 4 weeks, but not later time points, after the LDR priming. Data presented in Fig. 15 were processed to calculate slopes of fast (1-6 h) and slow (6-24 h) DSB repair kinetics components using pATM and gH2AX as markers of gross DSB. LDR exposure resulted in the acceleration of fast repair and deceleration of slow repair in pATM and gH2AX foci at 4 weeks post-irradiation with priming doses; however the net effect as evident from the number of residual foci at 24h was not affected in any of the exposure groups. Comparisons were made using two-way ANOVA (Tukey's method). *, ** and *** mark statistical significance at $p<0.05$, <0.01 and <0.001, respectively

3.4.3: Assessment of DSB repair capacity with γH2AX *and pATM proteins in HSKM*

The investigation of this mechanism in the primary human cells did not reveal a different pattern from what was discovered in the mouse myoblasts. In this model, foci induction only was used as an index for measuring repair capacity and the results in Fig. 17 showed no changes in pATM foci induction and residual DSB level but slight changes in gH2AX with LDR.

2 weeks

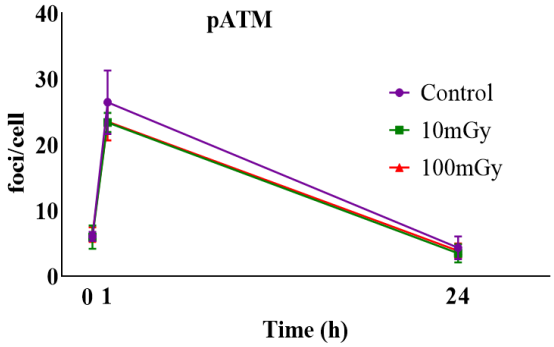
pATM
foci/cell
40
30
20
10
0
0 1
24
Time (h)
Control
10mGy
100mGy

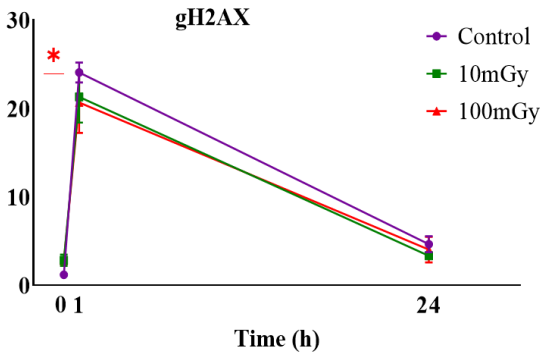
gH2AX
*
30
20
10
0
0 1
24
Time (h)
Control
10mGy
100mGy

Fig. 17: Exposure of HSKM myoblasts to LDR at early passages does not change cells ability to detect and repair exogenously induced DSB. Cells were exposed to priming gamma-irradiation at doses of 0 (Control), 10 or 100 mGy at t=0 and maintained by routine subculturing under normal growth conditions. At 0 and 2 weeks post-priming, cells were challenged with a high dose of 2000 mGy and the induced DSB were visualized as and scored as pATM (A) and γH2AX (B) foci using immuno-fluorescence microscopy at 0, 1 and 24h post-challenge. Number of foci per cell was quantified and plotted resulting in foci repair curves. Although, a slight statistical significance with γH2AX foci induction was observed in 100mGy exposed cells, overall, there were no differences between the control and LDR primed groups, indicating the lack of the effect of LDR on the cells ability to detect and repair gross DSB after a high-dose challenge. Exposure groups are color coded: sham irradiated, purple, 10mGy, green and 100mGy, red. Data are means of three independent experiments, with over 100 nuclei per data point scored in each biological replicate. Comparisons were done using Student's paired one-tailed t-test. Color coding of statistical significance signify comparisons between corresponding treatment groups and time-matched control. ** mark statistical significance at <0.01.

3.5. LDR produced a slight shift towards the HR pathway

3.5.1: Involvement of HR and NHEJ pathways in the repair of DSB

Given the complexities of DSB repair, it is therefore important to understand the intricate regulation of the DDR upon DSB formation [158]. Disappearance of foci during some time after the induction of DSB does not necessarily mean accurate repair. The accuracy of DSB repair is determined by the choice of repair pathway, which in this study includes the two main pathways: HR and NHEJ. HR is characterised as error-free and NHEJ in contrast is error-prone. They were assessed and analyzed using Rad51 and 53BP1 foci, respectively. Measurement and quantification of Rad51 and 53BP1 foci was carried out using the same conditions and in the same samples as the measurement of pATM and γH2AX foci.

3.5.2: Assessment of LDR-induced changes in HR and NHEJ in C2C12 cells

The involvement of HR and NHEJ in C2C12 cells was assessed using Rad51 and 53BP1 antibodies respectively in cells exposed to a challenging high dose of 2000mGy that is expected to result in 50-80 DSB per cell. The activity of each pathway was examined by using the same parameters as applied in the measurement of DSB repair capacity by pATM and γH2AX (Section 3.4.2). The frequency of each pathway was then determined using the fast (slope 1-6h) and slow (slope 6-24h) repair kinetics and the completion of repair (residual foci levels at 24h). It was assumed that fast repair by HR and slow repair by NHEJ suggest more accurate repair potentially causing beneficial outcomes.

The priming of myoblasts with LDR did not produce any evident changes in the 53BP1 foci except for a transient modulation detected at 4 weeks. The graph in Fig. 19b shows a slight suppression of fast repair component with LDR. Asides this, the rate of fast repair was not dependent on age or

radiation dose. Slow repair component, on the other hand, was slightly enhanced with LDR. Even though the differences were non-significant, the LDR-exposed population displayed a trend of higher NHEJ activity during the slow phase of repair compared to the control. The overall residual levels of 53BP1 foci were unaffected by LDR.

Although changes in HR kinetics looked more drastic compared to NHEJ, the changes were predominantly not significant, yet the trend suggests activation of the HR repair by LDR (Figure 18b). At 0 and 4 weeks, a delayed activation of HR was seen in non-LDR control cells as evident from a delayed peak of Rad51 foci at 6h, as opposed to normally observed maximum at 1h. Even though this shift was not observed in the subsequent weeks of analysis, the trend of lower activation at 1h in non-LDR control compared to LDR primed cells was observed throughout the study. Contrary to the observed trend with NHEJ, the enhancement of fast repair and suppression of slow repair for HR was induced by LDR priming. Similar to NHEJ, residual HR foci levels were not affected by LDR.

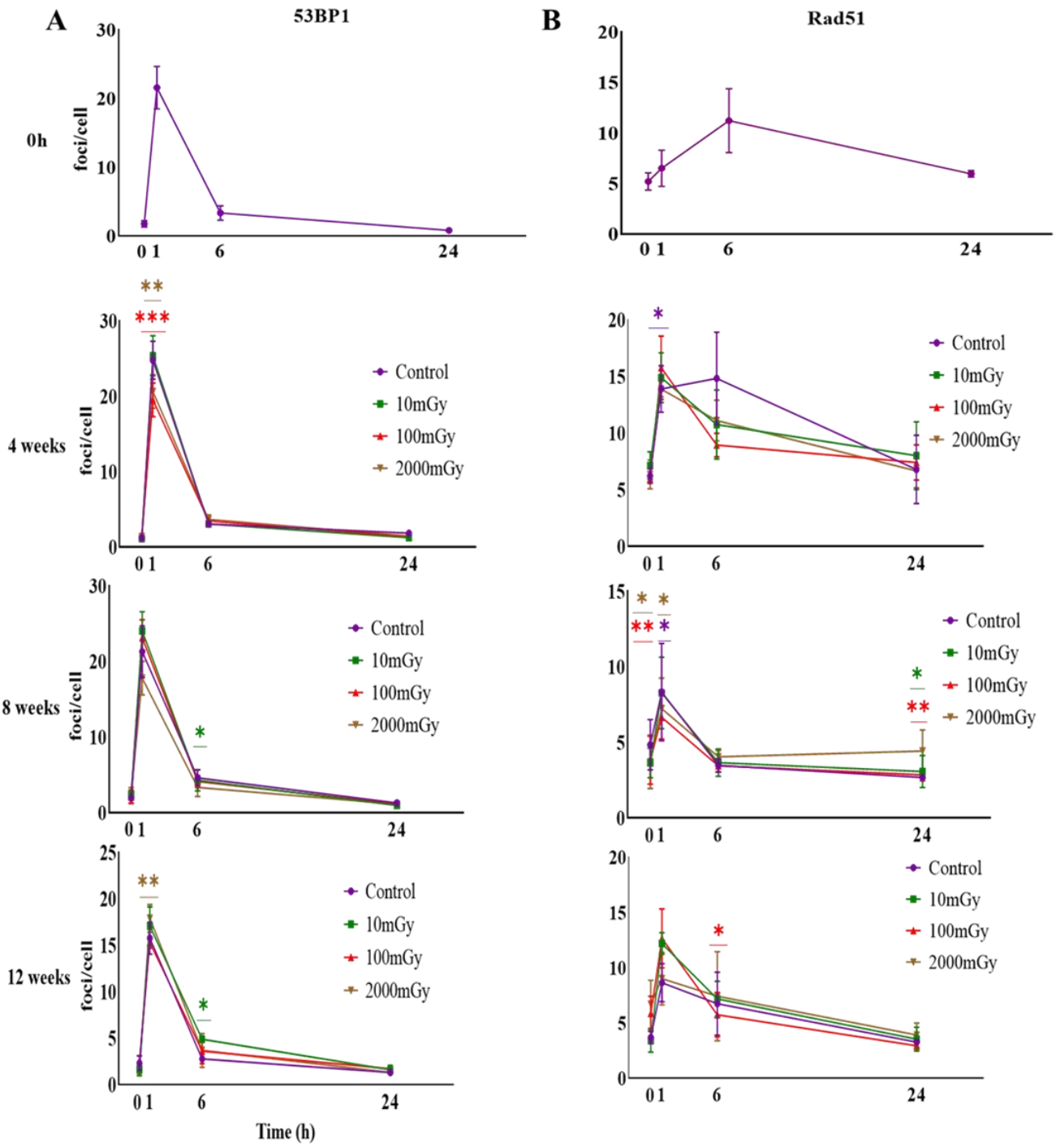
A
53BP1
B
Rad51
0h
4 weeks
8 weeks
12 weeks
foci/cell
Time (h)
Control
10mGy
100mGy
2000mGy

Fig. 18: Exposure of C2C12 myoblasts to LDR at early passages affects the HR pathway to a greater extent than it does the NHEJ pathway. Cells were exposed to priming gamma-irradiation at doses of 0 (Control), 10, 100 or 2000 mGy at t=0 and maintained by routine subculturing under normal growth conditions. At 0, 4, 8 and 12 weeks post-priming, cells were challenged with a high dose of 2000 mGy and the response of NHEJ or HR to the induced DSB were examined by visualizing and scoring 53BP1 (A) or γH2AX (B) foci, respectively, using immuno-fluorescence microscopy at 0, 1, 6 and 24h post-challenge. Number of foci per cell was quantified and plotted resulting in foci repair curves. Although, statistical significance was observed between select exposure groups for some time points, overall, the differences are sporadic, indicating the lack of the effect of LDR on the cells ability to activate NHEJ. In contrast, more substantial changes are seen in the kinetics of the HR marker Rad51. Exposure groups are color coded: sham irradiated, purple, 10mGy, green, 100mGy, red and 2000mGy, brown. Data are means of three independent experiments, with over 100 nuclei per data point scored in each biological replicate. Comparisons were done using Student's paired one-tailed t-test. Color coding of statistical significance signify comparisons between corresponding treatment groups and time-matched control. *, ** and *** mark statistical significance at $p<0.05$, <0.01 and <0.001, respectively.

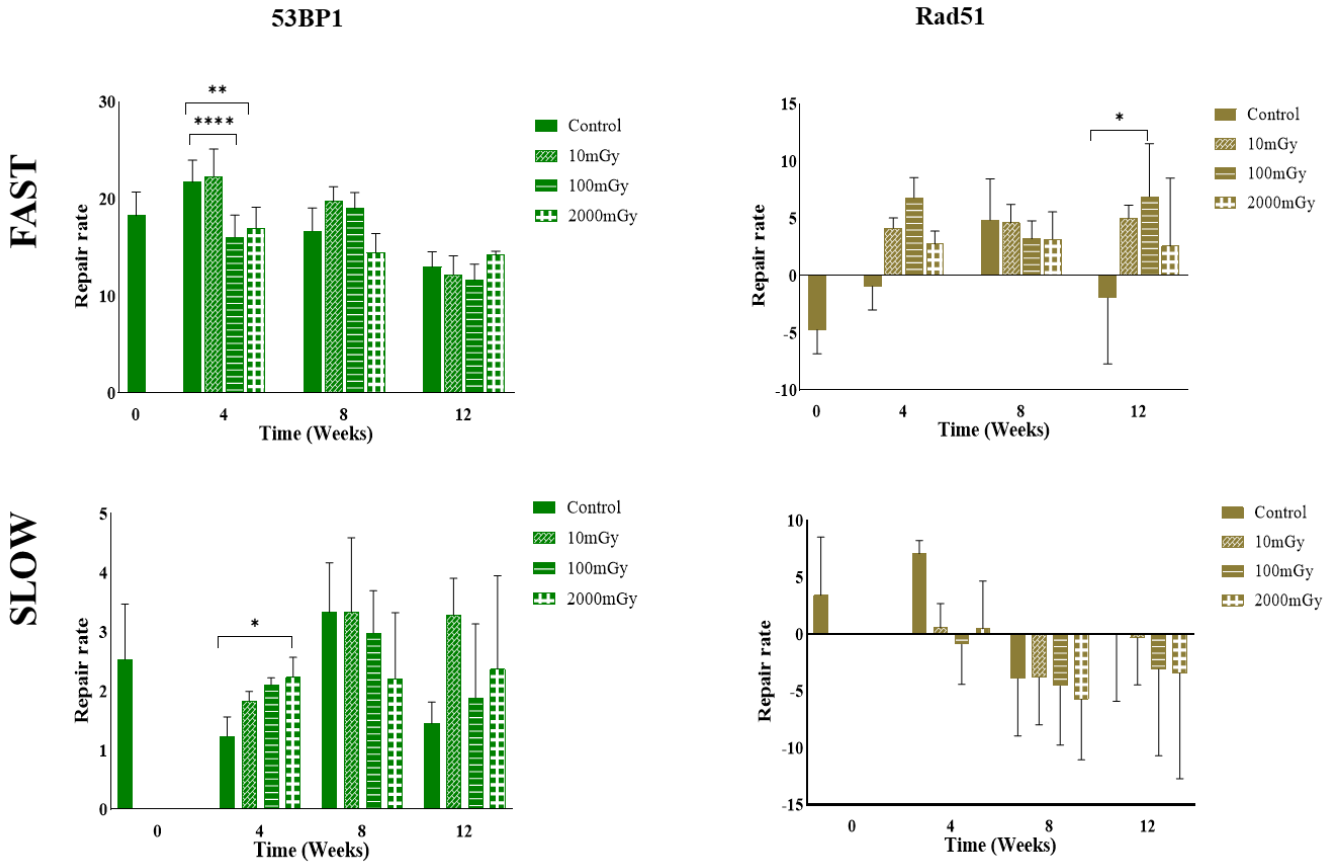
53BP1
Rad51
FAST
SLOW
Repair rate
Time (Weeks)
Control
10mGy
100mGy
2000mGy
**
****
*
0
4
8
12

Fig. 19: Exposure of C2C12 myoblasts to LDR at early passages differentially affects NHEJ vs HR repair components. Data presented in Fig. 18 were processed to calculate slopes of fast (1-6 h) and slow (6-24 h) repair kinetics components using 53BP1 and Rad51 as markers of NHEJ and HR, respectively. LDR exposure resulted in mild redistribution of DSB repair by NHEJ between the fast and slow kinetics components at 4 and 12 weeks post-priming (A). Although non-significant, a trend of enhanced fast repair and suppressed slow repair in LDR-exposed cells is seen for the HR pathway (B). Comparisons were made using two-way ANOVA (Tukey's method). *, ** and *** mark statistical significance at $p<0.05$, <0.01 and <0.001, respectively

3.5.3 Assessment of LDR-induced activity of HR and NHEJ in HSKM

HSKM cells were assessed for HR/NHEJ repair responses in a manner similar to that used for C2C12 cells, except for the lack of a 6h time point. Cells were primed with 0, 10 and 100mGy at time=0 and exposed to a challenge dose of 2000mGy at week 2. Foci induction and residual levels of foci were measured to compare the ratio of HR to NHEJ.

In HSKM cells a stronger induction of Rad51 foci was seen in 100 mGy treated cells at 1h after the 2000mGy challenge (Fig. 20b) compared to control cells. However, residual foci did not differ from those in the control untreated cells. No differences in 53BP1 foci kinetics were found in human myoblasts between control and LDR-treated cells.

Results thus far indicate that no drastic changes in the DSB related end-points were produced by LDR in HSKM cells. Changes were low in magnitude, not very consistent throughout the time points and doses. Among the trends, relative activation of HR vs. NHEJ can be noted.

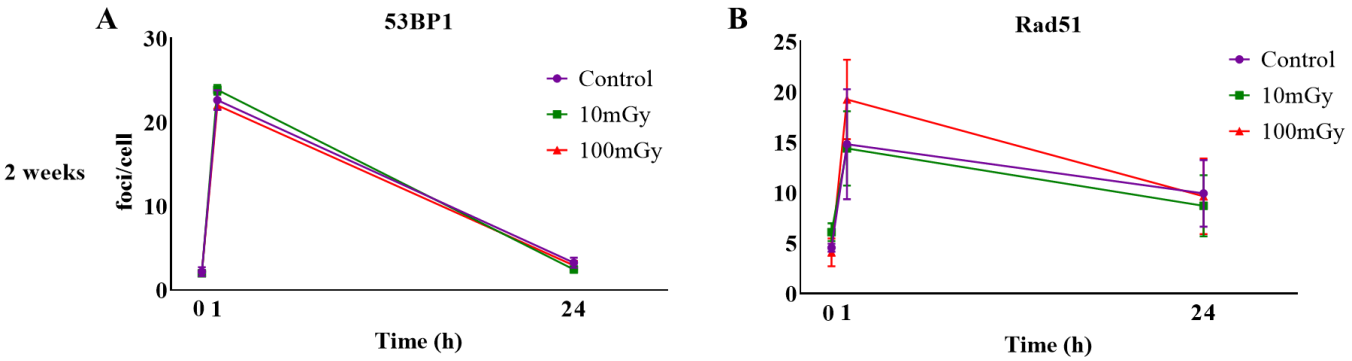
A
53BP1
2 weeks
foci/cell
30
20
10
0
0 1
24
Time (h)
Control
10mGy
100mGy
B
Rad51
25
20
15
10
5
0
0 1
24
Time (h)
Control
10mGy
100mGy

Fig. 20: Exposure of HSKM myoblasts to LDR at early passages affects neither the HR nor NHEJ pathway. Cells were exposed to priming gamma-irradiation at doses of 0 (Control), 10 or 100mGy at t=0 and maintained by routine subculturing under normal growth conditions. At 0 and 2 weeks post-priming, cells were challenged with a high dose of 2000 mGy and the response of NHEJ or HR to the induced DSB were examined by visualizing and scoring 53BP1 (A) or γH2AX (B) foci, respectively, using immuno-fluorescence microscopy at 0, 1 and 24h post-challenge. Number of foci per cell was quantified and plotted resulting in foci repair curves. Although non-significant, 100mGY exposed cells displayed a trend of better induction of HR foci. Asides this, no statistical significance was observed between treatment groups at all time points, indicating a weak effect of LDR on the preferred activation of HR in the HSKM model. Exposure groups are color coded: sham irradiated, purple, 10mGy, green, 100mGy, red. Data are means of three independent experiments, with over 100 nuclei per data point scored in each biological replicate. Comparisons were done using Student's paired one-tailed t-test. Color coding of statistical significance signify comparisons between corresponding treatment groups and time-matched control.

3.5.4 Effects of LDR on NHEJ: HR ratio in muscle myoblasts

To get a better insight into relative contributions of NHEJ vs. HR in repair of DSB, the two end points were put in a single perspective by evaluating the fractions of DSB processed by the two pathways. For this, total numbers of DSB were derived as means of γH2AX and pATM foci, followed by the calculation of percent Rad51 or 53BP1 foci relative to the total DSB number. The calculated NHEJ and HR fractions were then normalized to 100% since the sum of Rad51 and 53BP1 foci typically exceeded the number of the total number of DSB possibly due to co-localisation of a small fraction of Rad51 and 53BP1 foci.

The results showed that the ratio of NHEJ: HR was consistently high, expectedly suggesting more involvement of NHEJ than HR in DSB repair (Fig. 21). This balance was not affected by irradiation at time-points of 4 or 8 weeks. However, at 12 week, LDR-treated cells displayed a slight shift towards HR. A similar shift was seen in 100mGy-treated HSKM cells.

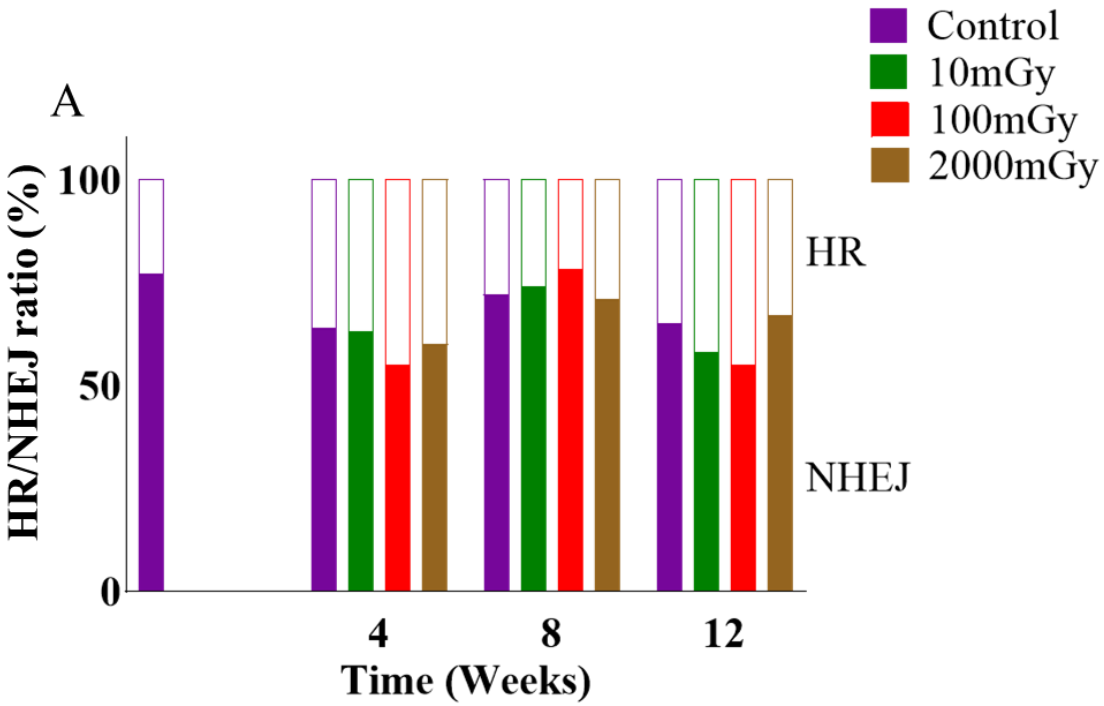
A
Control
10mGy
100mGy
2000mGy
HR/NHEJ ratio (%)
100
50
0
HR
NHEJ
4
8
12
Time (Weeks)

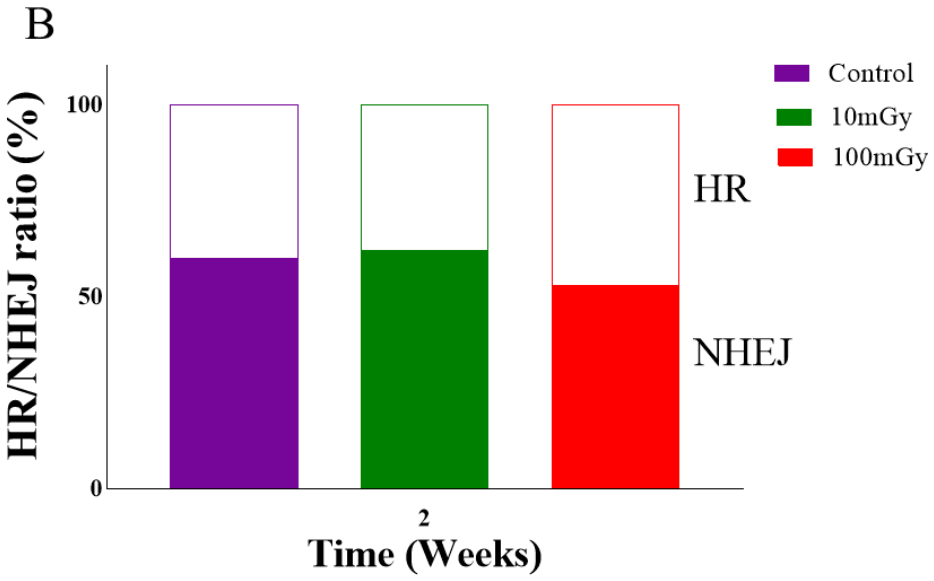
B
Control
10mGy
100mGy
HR/NHEJ ratio (%)
100
50
0
HR
NHEJ
2
Time (Weeks)

Fig. 21: Exposure of mouse (A) or human (B) myoblasts to LDR at early passages tends to make cells preferentially activate HR vs NHEJ pathway. HR/NHEJ ratio was calculated using 53BP1 (NHEJ) or Rad51 (HR) foci numbers at 1h after a challenging 2000mGy exposure and percent of total number of DSB (the mean of γH2AX and pATM foci) at 1h was plotted. The ratio of HR to NHEJ was slightly affected in LDR-exposed C2C12 cells, shifting the balance towards HR at 12 weeks post-priming. A similar shift is seen in 100mGy exposed human HSKM cells.

CHAPTER 4: DISCUSSION

In recent years, stem cells have shown significant implications for the progress in many fields of biotechnology, including cell-based regenerative therapies, drug testing and screening, and disease modeling in radiotherapy [161]. However, the success of this technology, like most we have seen, could be threatened by potential side effects, if not properly understood and managed. Given the persistence of stem cells in the body [162], stem cells may undergo several rounds of intrinsic and extrinsic stresses. This possibility has given rise to a growing interest in the biological response of stem cells to radiation [163] and generated significant evidence on the carcinogenic risks associated with high dose radiation.

This study was undertaken to contribute to mechanistic understanding of the effects of LDR on the functionality of stem cells. Here, the effects of LDR on muscle stem cells were investigated to examine mechanisms underlying the beneficial effects of discovered in a previous study by CNL researchers. The results from that study, in line with this study, revealed an LDR-induced improvement of myogenic capacity, which is known to decline with age under normal conditions. This is consistent with documented beneficial effects LDR in cells [14, 15], particularly, stem cells [164, 165]. The responses triggered by LDR depend on the cell type since certain cells have displayed neither benefits nor detriment [21, 22] and some - detriment [163]. It was observed that the myogenic capacity of HSKM expressed as the ability to fuse into muscle fibers was substantially lower than in C2C12 cells. This may explain the lower response (statistically insignificant improvement) of HSKM cells to LDR in reversing the aging related loss of the myogenic capacity. Another study by F. Parker et al [166] displayed similar trend of HSKM with the least efficient ability to fuse. This implies that the extent to which each of the different types of cultured cells

(C2C12 and HSKM) can fuse and differentiate is largely determined by the intrinsic properties of these cells.

To investigate the sensitivity of stem cell function to LDR, γH2AX foci were quantified as well as the formation of micronuclei and anaphase bridges to assess the aging related changes in GI and how these can be influenced by LDR. The results showed that LDR-treated cells had lower rates of GI, suggesting that the observed enhancement of myogenic fiber formation in aged myoblasts might be associated with suppressed GI. Indeed, execution of the myogenic differentiation program is an extremely complex process involving large scale gene expression changes operated by genetic and epigenetic controlling pathways [167]. It is feasible to suggest that aging-related accumulation of genomic damage may affect cell's ability to accurately execute such a complex program. Epigenetic changes, accumulation of DNA damage and defective DNA repair have been reported to contribute to aging related declines [168]. Therefore, suppressing GI in long term culture of myoblasts is expected to improve the functional myogenic properties of these cells. This is consistent with the first portion of the results of this study showing concomitant improvement of the myogenic potential and the suppression of GI in LDR-treated long-term culture of myoblasts. The next step of the study was to elucidate what particular DNA integrity pathways contribute to the observed LDR-induced genome stabilization. DNA repair mechanisms were legitimate candidates to test for the involvement. This next step was initiated by screening the expression of 84 genes playing key roles in various DNA repair pathways. Their expression was measured using RT-qPCR and the data showed an overall activation of most repair pathways at 4 weeks post-LDR. Even though this effect did not last for the entire 12 weeks of observation with the upregulation of most genes disappearing, the data might be suggestive of some kind of a LDR-induced memory that can render better capacity to repair additional damage.

A few studies were carried out to investigate the involvement of both non-homologous end joining (NHEJ) and base excision repair (BER) genes and proteins in human PBMC under radiation adaptive response settings [169, 170]. These results showed the overexpression of some BER and NHEJ genes and proteins in primed resting PBMCs, but there was no information on the primed effects of LDR on HR-related gene expression. My study, however, investigated the impact that LDR could have in selectively upregulating the expression of genes associated with the error-free repair pathway. The results, which demonstrated better overexpression of HR genes compared to NHEJ following LDR exposure, suggests that LDR increases the activity of error-free repair and this may play a role in improving the integrity of the genome.

Msh4, Rpa1, Top3a and Xrcc5 were the only modulated genes in the 12-week old LDR-exposed culture. DNA mismatch repair is a highly conserved biological pathway that plays a key role in maintaining genomic stability [171]. Msh4, a mismatch gene, XRCC5, a gene involved in NHEJ repair and RPA1 and TOP3A genes associated with HR repair remained expressed at 12 weeks. Importantly, there were more upregulated genes at 12 weeks that are involved in HR than those of the NHEJ.

Given the major contribution of DSB formation to the gross rearrangement of chromosomes in GI and the modulation of DSB repair genes at the gene expression level, in our next step we examined the changes in DSB formation and repair in LDR exposed myoblasts. pATM and γH2AX foci were used as markers of DSB. Firstly, the basal levels of DSB, defined here as the levels of DSB at prolonged periods of time after the initial irradiation without the acute challenge by 2000mGy, were monitored. Overall, basal levels of DSB were found to be mostly unaffected by the initial irradiation (Fig. 13), suggesting that whatever the mechanistic changes triggered by LDR are, they do not affect endogenously generated DSB. This is partially in line with the findings by S. Grudzenski et al.

showing that an inducible response by high dose is required for efficient repair and that LDR is insufficient to trigger damage and repair response [173]. The spectra of endogenous (basal level) and radiation induced DNA lesions are very distinct, with the former characterized by the presence of complex DSB and multiple lesions within close proximity of each other called clustered lesions. Therefore, to fully evaluate the ability of cells to repair DSB, a high dose challenge is frequently used. When we used a 2000 mGy acute challenging irradiation, followed by examining DNA repair foci at 1hr, 6 and 24 h (1h and 24h for HSKM cells), we were able to evaluate the DSB repair capacity of LDR-exposed myoblasts to cope with a high-level damage. Similar to basal DSB levels, LDR primed cells did not exhibit an enhanced DSB repair capacity (Fig. 15). This is consistent with Blimkie et al [174], showing that DSB repair is not modulated in splenocytes and thymocytes of mice treated with 20 or 100mGy of gamma-radiation in vivo. It has also been reported that LDR-induced adaptive responses could protect cells from challenging high radiation dose-induced cell killing [175]. In our study, variability in fast and slow repair rates was observed across the weeks with data at 4 weeks displaying better fast repair of pATM foci and no modulation in subsequent weeks compared to control. This is consistent with the earlier reports on high degree of variability in radiation adaptive responses between cell lines from different donors and in the direction and magnitude of the adaptive response at DNA damage level [176]. Contrary to a study that revealed reduction of γH2AX foci at 24 hours in the LDR-primed human salivary gland cells [177] my study on MuSCs displayed similar levels of residual foci between the control and LDR-exposed groups, hence, suggesting that LDR does not affect the completion of repair.

This set of results of our study suggests that LDR does not influence long-term DSB repair capacity, in spite of the fact that DSB-related gross chromosomal aberrations tended to be modulated by LDR.

Considering that complete removal of repair foci does not always imply accurate DSB repair, our attention turned to two distinct DSB repair pathways, HR and NHEJ, that are known to be error-free and error-prone, respectively. Following the examination of repair capacity and the observed variability of repair rate between unirradiated and LDR-treated groups, the involvement of HR vs NHEJ in the repair process was evaluated. The results showed that priming the myoblasts with LDR did not produce any evident changes in the induction of 53BP1 foci. On the other hand, HR kinetics looked more ambiguous with the sham-irradiated culture showing a degree of variability with age. However, the trend of activation at 1h suggests that LDR slightly influenced HR repair. A previous study showed that DSB were quickly repaired (at around 2 hours) by NHEJ and slowly repaired (at around 12 hours) by HR [178]. In this study, the fast and slow rates of repair for both pathways were determined. Results indicate slowing repair by NHEJ and accelerating repair by HR, suggesting better repair accuracy. Further, fast NHEJ repair component was not different between sham-irradiated and LDR groups, whereas the slow repair in LDR-exposed cells slightly enhanced at 12 weeks. Although, this is inconsistent with the results reported by Zhao et al. [179] who showed an LDR-induced enhancement of fast repair by NHEJ in human and mouse fibroblasts, the difference can possibly be related to a known distinction in DNA repair between stem and non-stem cells [98]. Following the evaluation of HR repair rates, I observed that, although non-significant, HR fast repair rate at weeks 4 and 12 was better in LDR-primed cells vs the control. It is worth pointing that this result is consistent with the observed higher gene expression levels of several HR genes at 4 and 12 weeks, providing stronger evidence of HR activation by LDR. The reduced activity of slow repair rate also depicted accelerated HR repair with LDR. Consistent with our results, a marked enhancement of DSB repair by HR and weak enhancement of DSB repair by NHEJ were observed after low-dose irradiation [180]. This contradicts results from the study by Wang Z. et al. that demonstrated LDR-induced enhancement of slow repair of DSB after 6 to 24 hours by HR [177].

These results suggest that the mechanisms of radiation adaptive responses are not uniform and can vary with the cell types and irradiation conditions.

Finally, in an attempt to obtain an overall view of relative activation of HR vs NHEJ upon challenging exposure and its dependence on dose and age of cell culture, the fractions of 53BP1 or Rad51 foci relative to the total number of DSBs at 1h post-2000mGy were quantified and plotted (Fig. 21). This broad view on the relative involvement of HR vs NHEJ shows a slight shift from NHEJ to HR with LDR at week 12 only. Changes seen at week 4 and 8 are less consistent and most likely represent a combination of biological and detection variabilities. Nonetheless, this is consistent with the majority of LDR-induced changes in HR and NHEJ repair parameters analyzed throughout the study. They suggest an insignificant trend towards the enhancement of HR at weeks 4 and 12 as opposed to week 8 when the changes were more variable and/or negligible.

CONCLUSION

Beneficial effects of LDR on functional capacity of muscle myoblasts was confirmed in mouse and primary human cells. As hypothesized, these changes were accompanied by the suppression of GI as revealed by scoring the rates of micronuclei and anaphase bridges. However, no pronounced changes in the overall DNA DSB repair capacity was revealed in LDR exposed cells. Nonetheless, a comprehensive examination of HR vs NHEJ DSB repair pathways, using gene expression and repair foci experiments, revealed a trend towards the preferential use of error-free HR vs error-prone NHEJ pathway in LDR-exposed mouse myoblasts. Consistent with this, higher levels of gene expression for HR (and for BER) were seen in LDR exposed cells compared to age-matched untreated controls. Since the magnitude of this change was rather low and sporadic throughout the

study, it is difficult to conclude whether this represents the driving mechanism behind the observed suppression of GI and enhanced retention of myogenic potential with age in myoblasts as a result of LDR exposure.

Overall, this study demonstrated for the first time that LDR may trigger genome-stabilizing mechanisms that can operate for a long time and suppress the aging related decline in myogenic differentiation capacity. No evidence was obtained in favor of the enhancement of overall DSB repair efficiency. However, using a multitude of tests, a trend was revealed yet weakly supported by statistical tests, towards more accurate HR repair as opposed to error-prone NHEJ in LDR-exposed cells.

The limitations of this study were the variabilities and sporadic changes in foci quantification results, which might partly be associated with sub-optimal detection of foci by the antibodies used in this study. Therefore, future investigation of low dose effects should involve the use of additional end points, such as whole genome sequencing for measuring mutational burden in LDR-exposed vs control cells, which was attempted but not completed within this graduate study, or the use of CRISPR-Cas9 technology to inactivate specifically HR or NHEJ in this cell models and examine the resulting effects on GI and myogenic potential in long-term LDR-exposed cultures .

References

1. Mu H, Sun J, Li L. et al. (2018). Ionizing Radiation Exposure: hazards, prevention and biomarker screening. Environ Sci Pollut Res., 25: 15294.

2. Radiation Damage to DNA: Techniques, Quantitation and Mechanisms. (1997). Radiation Research, 148(5): 481-522.

3. Liebre M.R., Gu J., Lu H., Shimazaki N., Tsai A.G. (2010). Nonhomologous DNA end joing (NHEJ) and chromosomal translocations in humans. Subcell Biochem; 50: 279-96.

4. Lieber MR. (2010). The mechanism of double-strand DNA break repair by the nonhomologous DNA end-joining pathway. Annu Rev Biochem., 79:181–211.

5. Calabrese E.J. (2015). An abuse of risk assessment: how regulatory agencies improperly adopted LNT for cancer risk assessment. Arch Toxicol.; 89: 647-648.

6. Cuttler J.M. (2010). Commentary on using LNT for radiation protection and risk assessment. Dose Response; 8: 378-383.

7. United Nations Scientific Committee on the Effects of Atomic Radiation (UNSCEAR). 2000. Sources and effects of ionizing radiation. UNSCEAR 2000 Report to the General Assembly, with Scientific Annexes. NY: United Nations.

8. Socol, Y., & Dobrzyński, L. (2015). Atomic Bomb Survivors Life-Span Study: Insufficient Statistical Power to Select Radiation Carcinogenesis Model. Dose-response: a publication of International Hormesis Society, 13(1),14-034.

9. Taylor LS (1980). Some non-scientific influences on radiation protection standards and practice. The 1980 Sievert Lecture. Health Phys. 39(6): 851-74

10. Feinendegen LE, Pollycove M, Neumann RD (2013). Hormesis by LDR effects: Low-dose cancer risk modeling must recognize up-regulation of protection. In: Baum RP, editor. (Ed.) Therapeutic Nuclear Medicine, Springer, 500 p.

11. Iyer R, Lehnert BE (2002). Low dose, low-LET ionizing radiation-induced radioadaptation and associated early responses in unirradiated cells. Mutat Res.; 503: 1–9.

12. Vares G, Wang B, Tanaka K, et al. (2006). Radiation-induced adaptive response with reference to evidence and significance: a review. Indian J Rad Res.; 3: 16–34.

13. Joiner MC, Marples B, Lambin P, Short SC, Turesson I (2001). Low dose hypersensitivity: current status and possible mechanisms. Int. J. Radiat.; 49 (2): 379-389

14. Chen M, Huang Q, Xu W, She C, Xie ZG, Mao YT, et al. (2014). Low-dose X-ray irradiation promotes osteoblast proliferation, differentiation and fracture healing. PLoS One, 9(8): e104016

15. Liang X, Gu J, Yu D, Wang G, Zhou L, Zhang X, et al. (2016). Low-Dose Radiation Induces Cell Proliferation in Human Embryonic Lung Fibroblasts but not in Lung Cancer Cells: Importance of ERK1/2 and AKT Signaling Pathways. Dose Response;14(1):1559325815622174

16. Hooker AM, Bhat M, Day TK, Lane JM, Swinburne SJ, Morley AA, et al. (2004). The linear no-threshold model does not hold for low-dose ionizing radiation. Radiat Res., 162(4): 447–52.

17. Jolly D, Meyer J. (2009). A brief review of radiation hormesis. Australas Phys Eng Sci Med., 32(4): 180–7.

18. Matsumoto H, Hamada N, Takahashi A, Kobayashi Y, Ohnishi T. (2007). Vanguards of paradigm shift in radiation biology: radiation-induced adaptive and bystander responses. J Radiat Res.; 48(2):97-106.

19. Kadhim M, Salomaa S, Wright E, Hildebrandt G, Belyakov OV, Prise KM, et al. (2012). Non-targeted effects of ionising radiation-Implications for low dose risk. Mutat Res.; 752(2): 84-98

20. Guéguen Y, Bontemps A, Ebrahimian TG (2019). Cell Mol Life Sci. 76(7):1255-1273.

21. Kiuru A, Kamarainen M, Heinavaara S, Pylkas K, Chapman K, Koivistoinen A, et al. (2014). Assessment of targeted and non-targeted responses in cells deficient in ATM function following exposure to low and high dose X-rays. PLoS One; 9(3): e93211

22. Jiang H, Xu Y, Li W, Ma K, Cai L, Wang G. (2008). Low-dose radiation does not induce proliferation in tumor cells in vitro and in vivo. Radiat Res.; 170(4): 477–87.

23. Li-Chun W., Yin-Xiu D, Yong-Hong L., Li D, Ya B., Mei S., Liang-Wei C. (2012). Low-Dose Radiation stimulates Wnt/Beta-Catenin signaling, neural stem cell proliferation and neurogenesis of the mouse hippocampus in vitro and in vivo. Curr. Alzheimer Res.; 9 (3): 278-289 (12).

24. Wiencke JK, Afzal V, Olivieri G, Wolff S. (1986). Evidence that the [3H]thymidine-induced adaptive response of human lymphocytes to subsequent doses of X-rays involves the induction of a chromosomal repair mechanism. Mutagenesis; 1: 375-80.

25. Ikushima T, Aritomi H, Morisita J. (1996). Radioadaptive response: efficient repair of radiation-induced DNA damage in adapted cells. Mutat Res.; 358: 193-8.

26. Otsuka K., Koana T., Tauchi H. and Sakai K. (2006). Activation of antioxidative enzymes induced by low-dose-rate whole-body gamma irradiation: adaptive response in terms of initial DNA damage, Radiat. Res. 166: 474-478.

27. Fan M., Ahmed K. M., Coleman M. C., Spitz D. R. and Li J. J. (2007). Nuclear factor-kappaB and manganese superoxide dismutase mediate adaptive radioresistance in low-dose irradiated mouse skin epithelial cells. Cancer Res. 67: 3220-3228.

28. Rothkamm K. and Löbrich M. (2003). Evidence for a lack of DNA double-strand break repair in human cells exposed to very low x-ray doses, Proc. Natl. Acad. Sci. USA 100: 5057-5062

29. Bucher N and Britten CD. (2008). G2 checkpoint abrogation and checkpoint kinase-1 targeting in the treatment of cancer. Br J Cancer 98: 523-528

30. Chapman, J. R., Taylor, M. R. G., and Boulton, S. J. (2012). Playing the end game: DNA double-strand break repair pathway choice. Mol. Cell, 47: 497–510.

31. Bakkenist CJ, Kastan MB. (2003). DNA damage activates ATM through intermolecular autophosphorylation and dimer dissociation. Nature, 421:499–506.

32. Rogakou EP, Pilch DR, Orr AH. et al. (1998) DNA double-stranded breaks induce histone H2AX phosphorylation on serine 139. J Biol Chem., 273:5858–5868.

33. Stewart GS, Wang B, Bignell CR. et al. (2003). MDC1 is a mediator of the mammalian DNA damage checkpoint. Nature, 421:961–966.

34. Wang B, Matsuoka S, Carpenter PB. et al. (2002). 53BP1, a mediator of the DNA damage checkpoint. Science, 298:1435–1438.

35. Haaf T, Golub EI, Reddy G. et al. (1995). Nuclear foci of mammalian Rad51 recombination protein in somatic cells after DNA damage and its localization in synaptonemal complexes. Proc Natl Acad Sci USA, 92:2298–2302.

36. Thompson LH, Limoli CL. Origin, Recognition, Signaling and Repair of DNA Double-Strand Breaks in Mammalian Cells. In: Madame Curie Bioscience Database [Internet]. Austin (TX): Landes Bioscience; 2000-2013.

37. Abraham RT. (2001). Cell cycle checkpoint signaling through the ATM and ATR kinases. Genes Dev., 15:2177–2196.

38. Durocher D, Jackson SP. (2001). DNA-PK, ATM and ATR as sensors of DNA damage: Variations on a theme? Curr Opin Cell Biol., 13:225–231.

39. Bakkenist, C.J. and Kastan M.B. (2003). DNA damage activates ATM through intermolecular autophosphorylation and dimer dissociation. Nature, **421**(6922): p. 499-506.

40. Rogakou EP, Boon C, Redon C. et al. (1999). Megabase chromatin domains involved in DNA double-strand breaks in vivo. J Cell Biol., 146:905–916.

41. Furuta T, Takemura H, Liao ZY. et al. (2003). Phosphorylation of histone H2AX and activation of Mre11, Rad50, and Nbs1 in response to replication-dependent DNA double-strand breaks Induced by mammalian DNA topoisomerase I cleavage complexes. J Biol Chem., 278:20303–20312.

42. Rogakou EP, Boone C, Redon C, Bonner WM. (1999). Megabase chromatin domains involved in DNA double-strand breaks in vivo. J. Cell Biol.; 146: 905–916.

43. Celeste A, et al. (2003). Histone H2AX phosphorylation is dispensable for the initial recognition of DNA breaks. Nat. Cell Biol.; 5: 675–679.

44. Pastink, A. and Lohman P.H.M. (1999). Repair and consequences of double-strand breaks in DNA. Mutation Research/Fundamental and Molecular Mechanisms of Mutagenesis, **428**(1): p. 141-156.

45. Natale, F., et al. (2017). Identification of the elementary structural units of the DNA damage response. Nature Communications, **8**(1): p. 15760.

46. Beucher, A., Birraux, J., Tchouandong, L., Barton, O., Shibata, A., Conrad, S., Goodarzi, A. A., Krempler, A., Jeggo, P. A., and Lobrich, M. (2009). ATM and Artemis promote homologous recombination of radiation -induced DNA double -strand breaks in G2. Embo J 28, 3413 -3427

47. Bothmer A, Robbiani DF, Di Virgilio M, Bunting SF, Klein IA, Feldhahn N, et al. (2011). Regulation of DNA end joining, resection, and immunoglobulin class switch recombination by 53BP1. Molecular Cell, 42(3): 319–29.

48. Mahaney BL, Meek K, Lees-Miller SP. (2009) Repair of ionizing radiation-induced DNA double-strand breaks by non-homologous end-joining. Biochem J., 417(3): 639–50.

49. Scott SP, Pandita TK. (2006). The cellular control of DNA double-strand breaks. J Cell Biochem., 99(6): 1463–75.

50. Pandita TK, Richardson C. (2009) Chromatin remodeling finds its place in the DNA double-strand break response. Nucleic Acids Res., 37(5):1363–77.

51. Kobayashi J, Iwabuchi K, Miyagawa K, et al. (2008). Current topics in DNA double strand break repair. J Radiat Res, 49: 93–103.

52. Symington LS, Gautier J. (2011). Double-strand break end resection and repair pathway choice. Annu Rev Genet., 45:247–71.

53. Baumann P, West SC. (1998). Role of the human Rad51 protein in homologous recombination and double-stranded-break repair. Trends Biochem Sci., 23: 247-51

54. Vispe S, Defais M (1997). Mammalian Rad51 protein: a RecA homologue with pleiotropic functions. Biochimie., 79: 587-92.

55. Panier, S. & Boulton, S. J. (2014). Double-strand break repair: 53BP1 comes into focus. *Nat. Rev. Mol. Cell Biol.* **15**, 7–18

56. Wang G. and Cai L. (2000). Induction of Cell-Proliferation Hormesis and Cell-Survival Adaptive Response in Mouse Hematopoietic Cells by Whole-Body Low-Dose Radiation. Toxicological Sciences; 53(2): 369–76.

57. Riballo E., Kuhne M., Rief N. et al. (2004). A pathway of double strand break joining dependent upon ATM, Artemis and proteins locating to gamma-H2AX foci. Mol. Cell, 16: 715-724

58. Shibata A, Conrad S, Birraux J, Geuting V, Barton O, Ismail A, et al. (2011). Factors determining DNA doublestrand break repair pathway choice in G2 phase. EMBO J.; 30: 1079–1092.

59. Escribano-Díaz, C. *et al.* A cell cycle-dependent regulatory circuit composed of 53BP1-RIF1 and BRCA1-CtIP controls DNA repair pathway choice. *Mol. Cell* **49**, 872–883 (2013)

60. Zimmermann, M., Lottersberger, F., Buonomo, S. B., Sfeir, A. and de Lange, T. (2013). 53BP1 regulates DSB repair using Rif1 to control 5′ end resection. *Science* **339**, 700–704.

61. Mao, Z., Bozzella, M., Seluanov, A., & Gorbunova, V. (2008). Comparison of nonhomologous end joining and homologous recombination in human cells. *DNA repair*, *7*(10), 1765–1771.

62. Johnson RD, Jasin M. (2000). Sister chromatid gene conversion is a prominent double strand break repair in mammalian cells. EMBO J.; 19: 3398–3407.

63. Haber J. E. (2014). Genome Stability: DNA Repair and Recombination. New York, NY: Garland Science

64. Hashimoto Y., Chaudhuri A. R., Lopes M., Costanzo V. (2010). Rad51 protects nascent DNA from MRE11-dependent degradation and promotes continuous DNA synthesis. Nat. Struct. Mol. Biol. 7, 1305–1311

65. Betermier M, Bertrand P, Lopez BS. (2014) Is non-homologous end-joining really an inherently error-prone process? PLoS Genet.; 10(1)

66. Li X, Heyer WD. (2008). Homologous recombination in DNA repair and DNA damage tolerance. Cell Res.; 18: 99–113.

67. Bhattacharjee, S., & Nandi, S. (2016). Choices have consequences: the nexus between DNA repair pathways and genomic instability in cancer. *Clinical and translational medicine*, *5*(1), 45.

68. Syeda AH, Hawkins M, McGlynn P. (2014). Recombination and replication. Cold Spring Harb Perspect Biol.; 6(11): a016550.

69. Difilippantonio MJ et al (2000) DNA repair protein Ku80 suppresses chromosomal aberrations and malignant transformation. Nature 404(6777):510–514

70. Yan CT, Boboila C, Souza EK, Franco S, Hickernell TR, et al. (2007) IgH class switching and translocations use a robust non-classical end-joining pathway. Nature 449: 478–482.

71. Boboila C, Jankovic M, Yan CT, Wang JH, Wesemann DR, et al. (2010) Alternative end-joining catalyzes robust IgH locus deletions and translocations in the combined absence of ligase 4 and Ku70. Proc Natl Acad Sci U S A 107: 3034–3039.

72. Gao Y, Ferguson DO, Xie W, Manis JP, Sekiguchi J, et al. (2000) Interplay of p53 and DNA-repair protein XRCC4 in tumorigenesis, genomic stability and development. Nature 404: 897–900.

73. Rothkamm K., Kuhne M., Jeggo P.A., Lobrich M. (2001). Radiation-induced genomic rearrangements formed by nonhomologous end-joining of DNA double-strand breaks. Cancer Res.; 61: 3886–3893.

74. Weinstock D.M., Richardson C.A., Elliott B., Jasin M. (2006). Modeling oncogenic translocations: Distinct roles for double-strand break repair pathways in translocation formation in mammalian cells. DNA Repair.; 5: 1065–1074.

75. Lieber M.R., Gu J., Lu H., Shimazaki N., Tsai A.G. (2010). Nonhomologous DNA end joining (NHEJ) and chromosomal translocations in humans. Subcell. Biochem.; 50: 279–296.

76. Ghezraoui H., Piganeau M., Renouf B., Renaud J.B., Sallmyr A., Ruis B., Oh S., Tomkinson A.E., Hendrickson E.A., Giovannangeli C., et al. (2014). Chromosomal translocations in human cells are generated by canonical nonhomologous end-joining. Mol. Cell.; 55: 829–842.

77. Adamo A., Collis S.J., Adelman C.A., Silva N., Horejsi Z., Ward J.D., Martinez-Perez E., Boulton S.J., La Volpe A. (2010). Preventing nonhomologous end joining suppresses DNA repair defects of Fanconi anemia. Mol. Cell.; 39: 25–35.

78. Pace P., Mosedale G., Hodskinson M.R., Rosado I.V., Sivasubramaniam M., Patel K.J. (2010). Ku70 corrupts DNA repair in the absence of the Fanconi anemia pathway. Science.; 329: 219–223.

79. Mujoo, K. et al. (2017). Differentiation of Human Induced Pluripotent or Embryonic Stem Cells Decreases the DNA Damage Repair by Homologous Recombination. *Stem cell reports*, *9*(5), 1660–1674.

80. Han, J., Ruan, C., Huen, M., Wang, J., Xie, A., Fu, C., and Huang, J. (2017). BRCA2 antagonizes classical and alternative nonhomologous end-joining to prevent gross genomic instability. *Nature communications*, *8*(1), 1470.

81. San Filippo J, Sung P, Klein H. (2008). Mechanism of eukaryotic homologous recombination. Annu Rev Biochem.; 77: 229–257.

82. Wiese C., Dray E., Groesser T., Filippo J.S., Shi I., Collins D.W., Tsai M.S., Williams G.J., Rydberg B., Sung P. and Schild D. (2007). Promotion of Homologous Recombination and Genomic Stability by Rad51APA via Rad51 Recombinase Enhancement. Molecular Cell., 28(3):482-490

83. Magdalou I, Lopez BS, Pasero P, Lambert SA. (2014). The causes of replication stress and their consequences on genome stability and cell fate. Semin Cell Dev Biol.; 30C: 154-64

84. Wilhelm, T., Magdalou, I., Barascu, A., Técher, H., Debatisse, M., & Lopez, B. S. (2014). Spontaneous slow replication fork progression elicits mitosis alterations in homologous recombination-deficient mammalian cells. *Proceedings of the National Academy of Sciences of the United States of America*, *111*(2), 763–768.

85. Lee E. S., Won Y. J., Kim B. C., Park D., Bae J. H., Park S. J., Son T. G. (2016). Low-dose irradiation promotes Rad51 expression by down-regulating miR-193b-3p in hepatocytes. *Scientific reports*, *6*, 25723.

86. Yatagai F, Suzuki M, Ishioka N, Ohmori H, Honma M Repair of I-SceI induced DSB at a specific site of chromosome in human cells: influence of low-dose, low-dose-rate gamma-rays. Radiat Environ Biophys2008;47: 439–444.

87. Jaklenec A, Stamp A, Deweerd E, Sherwin A, Langer R (2012). Progress in the tissue engineering and stem cell industry “are we there yet?”. Tissue Eng Part B Rev.; 18(3): 155–166.

88. Bailey AM, Mendicino M, Au P (2014). An FDA perspective on preclinical development of cell-based regenerative medicine products. Nat Biotechnol.; 32(8): 721–723.

89. Leahy M., Thompson K., Zafar H., Alexandrov S. et al. (2016). Functional Imaging for Regenerative Medicine; 7: 57

90. Kitahara CM, Linet MS, Rajaraman P, Ntowe E, Berrington de González A. (2015) A new era of low-dose radiation epidemilogy. Curr Environ Health Rep.; 2:236–249.

91. Xinyue Liang, You Ho So, Jiuwei Cui, Kewei Ma, Xiaoyi Xu, Yuguang Zhao, Lu Cai, Wei Li (2011). The Low-dose Ionizing Radiation Stimulates Cell Proliferation via Activation of the MAPK/ERK Pathway in Rat Cultured Mesenchymal Stem Cells. Journal of Radiation Research; 52 (3): 380–386

92. Wu B., Wei Y., Liu F.Q., Zhang Q., Wang C.B. and Bai H. (2011). Biological effects of low dose X-irradiation on human bone marrow mesenchymal stem cells. Zhongguo Shi Yan Xue Ye Xue Za Zhi; 19(5): 1214-7.

93. Li W., Wang G., Cui J., Xue L., and Cai L. (2004). Low-Dose Radiation (LDR) Induces Hematopoietic Hormesis: LDR-Induced Mobilization of Hematopoietic Progenitor Cells into Peripheral Blood Circulation. Experimental Hematology; 32(11): 1088–96.

94. Guo W., Wang G., Wang P., Chen Q., Tan Y. and Cai L. (2010). Acceleration of Diabetic Wound Healing by Low-Dose Radiation Is Associated with Peripheral Mobilization of Bone Marrow Stem Cells. Radiation Research; 174(4): 467–79.

95. Ishizaki K., Hayashi Y., Nakamura H., Yasui Y., Komatsu K., Tachibana A. (2004). No induction of p53 phosphorylation and few focus formations of phosphorylated H2AX suggest efficient repair of DNA damage during chronic low-dose-rate irradiation in human cells. J Radiat Res; 45:521–525.

96. Reya T., Morrison S. J., Clarke M. F., Weissman I. L. (2011). Stem cells, cancer, and cancer stem cells. *Nature*; 414(6859): 105–111.

97. Squillaro T., Alessio N., Di Bernardo G., Ozcan S., Peluso G. and Galderisi U. (2018). Stem cells and DNA repair capacity: Muse Stem cells are among the best performers. Adv. Exp. Med. Bio.; 1103: 103-113

98. Jacobs K.M., Misri S., Meyer B., Raj S., Zobel C.L., Sleckman B.P., Hallahan D.E., Sharma G.G. (2016). Unique epigenetic influence of H2AX phosphorylation and H3K56 acetylation on normal stem cell radioresponses. Mol. Biol. Cell.; 27: 1332–1345.

99. Sugrue T., Brown J.A., Lowndes N.F., Ceredig R. (2013). Multiple facets of the DNA damage response contribute to the radioresistance of mouse mesenchymal stromal cell lines. Stem Cells.; 31: 137–145.

100. Solier S., Pommier Y. (2011). MDC1 cleavage by caspase-3: A novel mechanism for inactivating the DNA damage response during apoptosis. Cancer Res.; 71: 906–913.

101. Tichy ED, Stambrook PJ (2008) DNA repair in murine embryonic stem cells and differentiated cells. Exp Cell Res 314(9):1929–1936

102. Savatier P et al (2002) Analysis of the cell cycle in mouse embryonic stem cells. Methods Mol Biol 185:27–33

103. Francis R, Richardson C (2007) Multipotent hematopoietic cells susceptible to alternative double-strand break repair pathways that promote genome rearrangements. Genes Dev 21(9):1064–1074

104. Blanpain, C., Mohrin, M., Sotiropoulou, P.A. and Passegué, E. (2011) DNA-damage response in tissue-specific and cancer stem cells. Cell Stem Cell 8:16–29.

105. Grewenig A., Schuler N., Rübe E.C. (2015). Persistent DNA damage in spermatogonial stem cells stem cells after fractionated low-dose irradiation of testicular tissue. Int. J. Radiation Oncol. Biol. Phys.; 92(5): 1-9.

106. Tsvetkova, A., Ozerov, I. V., Pustovalova, M., Grekhova, A., Eremin, P., Vorobyeva, N., … Osipov, A. N. (2017). γH2AX, 53BP1 and Rad51 protein foci changes in mesenchymal stem cells during prolonged X-ray irradiation. *Oncotarget*, *8*(38), 64317–64329

107. Sergeeva, V. A., Ershova, E. S., Veiko, N. N., Malinovskaya, E. M., Kalyanov, A. A., Kameneva, L. V., Stukalov, S. V., Dolgikh, O. A., Konkova, M. S., Ermakov, A. V., Veiko, V. P., Izhevskaya, V. L., Kutsev, S. I., … Kostyuk, S. V. (2017). Low-Dose Ionizing Radiation Affects Mesenchymal Stem Cells via Extracellular Oxidized Cell-Free DNA: A Possible Mediator of Bystander Effect and Adaptive Response. *Oxidative medicine and cellular longevity*

108. Prakash, R., Zhang, Y., Feng, W., & Jasin, M. (2015). Homologous recombination and human health: the roles of BRCA1, BRCA2, and associated proteins. *Cold Spring Harbor perspectives in biology*, *7*(4), a016600.

109. Mauro, A. (1961). Satellite cell of skeletal muscle fibers. *J. Biophys. Biochem. Cytol.* **9**, 493–495.

110. Parker MH (2015). The altered fate of aging satellite cells is determined by signaling and epigenetic changes. *Front. Genet.* 6:59.

111. Sousa-Victor P., Garcia-Prat L. and Munos-Canoves P. (2018). New mechanisms driving muscle stem cell regenerative decline with aging. Int. J. Dev. Biol., 62: 583-590

112. Ahmed, A. S., Sheng, M. H., Wasnik, S., Baylink, D. J., & Lau, K. W. (2017). Effect of aging on stem cells. *World journal of experimental medicine*, *7*(1), 1–10.

113. García-Prat L, Sousa-Victor P, Muñoz-Cánoves P. (2013). Functional dysregulation of stem cells during aging: a focus on skeletal muscle stem cells. FEBS J.; 280: 4051–4062.

114. Hwang A.B., Brack A.S. (2018). Muscle Stem Cells and Aging. Curr. Top. Dev. Biol., 126: 299-322

115. Lamb M.J. (1984). The effect of radiation on the longevity of female *Drosophila subobscura*. J. Insect Physiol., 10: 487-497

116. Sacher G.A. (1963). Effect of X-rays on the survival of *Drosophila imagoes*. Physiol. Zool., 36: 295-311

117. Calabrese E.J., Baldwin L.A. (2000). The effects of gamma rays on longevity. Biogerontology, 1: 309-319

118. Caratero A., Courtade M., Bonnet L., Planel H., Caratero C. (1998). Effect of continuous gamma irradiation at a very low dose on the life span of mice. Gerontology, 44: 272-276

119. Hayakawa N., Ohtaki M., Ueoka H., Matsuura M., Munaka M., Kurihara M. (1989). Mortality statistics of major causes of death among atomic bomb survivors in Hiroshima Prefecture from 1968 to 1982. Hiroshima J. Med. Sci., 38: 53-67

120. Mine M., Okumura Y., Ichimaru M., Nakamura T., Kondo S. (1990). Apparently beneficial effect of low to intermediate doses of A-bomb radiation on human lifespan. Int. J. Radiat. Biol., 58: 1035-1043

121. Atkinson W.D., Law D.V., Bromley K.J., Inskip H.M. (2004). Mortality of employees of the United Kingdom Atomic Energy Authority, 1946-97. Occup. Environ. Med., 61: 577-585

122. Dublin LI, Spigelman M. (1948). Mortality of medical specialists, 1938–1942. J Am Med Dir Assoc.; 137(17): 1519–1524.

123. Le Y., Pack T (2019). LDR delays aging of human cells. Cytotherapy, 21(5): e15.

124. Masuda S., Hisamatsu T., Seko D., Urata Y., Goto S., Li T-S., Ono Y. (2015). Time- and dose-dependent effects of total-body ionizing radiation on muscle stem cells. Physiol Rep.; 3(4): e12377

125. Dhawan, J. and Rando T. (2006). Stem cells in postnatal myogenesis: Molecular mechanisms of satellite cell quiescence, activation and replenishment. Trends in cell biology. **15**: 666-73.

126. Yusuf, I. and Fruman, D.A. (2003) Regulation of quiescence in lymphocytes. Trends Immunol. 24, 380–386

127. Schultz, E. and McCormick, K.M. (1994) Skeletal muscle satellite cells. Rev. Physiol. Biochem. Pharmacol. 123, 213–257

128. Hawke, T.J. and Garry, D.J. (2001) Myogenic satellite cells: physiology to molecular biology. J. Appl. Physiol. 91, 534–551

129. Day K., Shefer G., Shearer A., et al. (2010). The depletion of skeletal muscle satellite cells with age is concomitant with reduced capacity of single progenitors to produce reserve progeny. Dev. Biol.; 340(2):330–343.

130. Leiter J.R., Anderson J.E. (2010). Satellite cells are increasingly refractory to activation by nitric oxide and stretch in aged mouse-muscle cultures. Int. J. Biochem. Cell Biol.; 42(1):132–136.

131. Webster C., Blau H.M. (1990). Accelerated age-related decline in replicative life-span of Duchenne muscular dystrophy myoblasts: implications for cell and gene therapy. Somat. Cell Mol. Genet.; 16: 557–565.

132. Banks GB, Chamberlain JS. (2008). The value of mammalian models for duchenne muscular dystrophy in developing therapeutic strategies. Curr Top Dev Biol., 84: 431–453.

133. Christensen JF, Jones LW, Andersen JL, Daugaard G, Rorth M, Hojman P. (2014). Muscle dysfunction in cancer patients. Ann Oncol.; 25:947–58.

134. Sacco, A., et al. (2010). Short Telomeres and Stem Cell Exhaustion Model Duchenne Muscular Dystrophy in mdx/mTR Mice. Cell, **143**(7): 1059-1071.

135. Wallengren O, Iresjo BM, Lundholm K, Bosaeus I. (2015). Loss of muscle mass in the end of life in patients with advanced cancer. Support Care Cancer; 23:79–86.

136. Yang X. (2012). Stem cell transplantation for treating Duchenne muscular dystrophy. Neural Regen. Res.; 7(22): 1744-1751.

137. Prosperi, E.; Stivala, L.A.; Sala, E.; Scovassi, A.I.; Bianchi, L. (1993). Proliferating Cell Nuclear Antigen Complex Formation Induced by ultraviolet irradiation in human quiescent fibroblasts as detected by immunostaining and flow cytometry. *Exp. Cell Res.*; *205*, 320–325.

138. Tsien, R.Y. (1998). The green fluorescent protein. *Ann. Rev. Biochem.*; *67*, 509–544.

139. Goodarzi AA, Jeggo PA (2012) Irradiation induced foci (IRIF) as a biomarker for radiosensitivity. Mutat Res 736: 39-47.

140. Lukas C., Bartek J., Lukas J. (2005). Imaging of protein movement induced by chromosomal breakage: tiny 'local' lesions pose great 'global' challenges. Chromosoma.; 114:146–154.

141. Belyaev IY (2010) Radiation-induced DNA repair foci: spatio-temporal aspects of formation, application for assessment of radiosensitivity and biological dosimetry. Mutat Res 704: 132-141.

142. Metzger L, Iliakis G. Kinetics of DNA double-strand break repair throughout the cell cycle as assayed by pulsed field gel electrophoresis in CHO cells. Int J Radiat Biol. 1991; 59:1325–39.

143. Hoeijmakers JH. (2009). DNA damage, aging, and cancer. N Engl J Med 361: 1475–1485.

144. Kirkwood TB. (2005). Understanding the odd science of aging. Cell 120: 437–447

145. Fishel ML, Vasko MR, Kelley MR. (2007). DNA repair in neurons: So, if they don't divide what's to repair? Mutat Res 614: 24–36.

146. Rulten SL, Caldecott KW. (2013). DNA strand break repair and neurodegeneration. DNA Repair (Amst) 12: 558–567.

147. Pustovalova M., Grekhova A…Osipov A.N. (2016). Accumulation of spontaneous gH2AX foci in long-term cultured mesenchymal stromal cells. Aging; 8(12): 3498-3506.

148. Day K., Shefer G., Shearer A., Yablonka-Reuveni Z. (2010). The depletion of skeletal muscle satellite cells with age is concomitant with reduced capacity of single progenitors to produce reserve progeny. Dev Biol.; 340(2):330-43.

149. Brack, A. S., & Muñoz-Cánoves, P. (2016). The ins and outs of muscle stem cell aging. *Skeletal muscle*, *6*, 1

150. Tubbs, A., & Nussenzweig, A. (2017). Endogenous DNA Damage as a Source of Genomic Instability in Cancer. *Cell*, *168*(4), 644–656.

151. Osipov L.N., Pustovalova M…Eremin I. (2015). Low doses of X-rays induce prolonged and ATM-independent persistence of gH2AX foci in human gingival mesenchymal stem cells. Oncotarget; 6(29): 27275-27287.

152. Loeb LA, Springgate CF, and Battula N (1974). Errors in DNA replication as a basis of malignant changes. Cancer Res. 34, 2311–2321.

153. Manhart, C. M., & Alani, E. (2016). Roles for mismatch repair family proteins in promoting meiotic crossing over. *DNA repair*, *38*, 84–93.

154. Sleeth K.M…..Helleday T. (2007). RPA mediates recombination repair during replication stress and is displaced from DNA by checkpoint signalling in human cells. *Journal of molecular biology*

155. Raynard, S., Bussen, W., and Sung, P. (2006). A double Holliday junction dissolvasome comprising BLM, topoisomerase IIIalpha, and BLAP75. J. Biol. Chem. 281, 13861–13864.

156. Taccioli G.E., Gottlieb T.M., Blunt T., Priestly A., Demengeot J., Mizuta R., Lehmann A.R., Alt F.W., Jackson S.P., Jeggo P.A. (1994). Ku80: product of the XRCC5 gene and its role in DNA repair and V(D)J recombination. Science; 265 (5177): 1442-5

157. Rogakou E.P., Pilch D.R., Orr A.H., Ivanova V.S., Bonner W.M. (1998). DNA double stranded breaks induce histone H2AX phosphorylation on serine 139. J. Biol. Chem. 273, 5858-5868.

158. Ivashkevich A., Redon C.E., Nakamura A.J., Martin R.F., Martin O.A. (2011). Use of the gH2AX assay to monitor DNA damage and repair in translational cancer research. Cancer Lett. 327, 123-133.

159. Jeggo P., Lavin M.F. (2009). Cellular radiosensitivity: how much better do we understand it? Int. J. Radiat. Biol.; 85: 1061-1081

160. Brandsma, I., & Gent, D. C. (2012). Pathway choice in DNA double strand break repair: observations of a balancing act. *Genome integrity*, *3*(1), 9.

161. Hur W., & Yoon S. K. (2017). Molecular Pathogenesis of Radiation-Induced Cell Toxicity in Stem Cells. International journal of molecular sciences, 18(12), 2749.

162. Signer R. A., & Morrison S. J. (2013). Mechanisms that regulate stem cell aging and life span. Cell stem cell, 12(2), 152–165.

163. Schröder A., Kriesen S., Hildebrandt G. and Manda K. (2019). First insights into the effects of low-dose X-ray Irradiation in Adipose-derived stem cells. Int. J. Mol. Sci., 20, 6075

164. Li W., Wang G., Cui J., Xue L., Cai L. (2004). LDR (LDR) induces hematopoietic hormesis: LDR-induced mobilization of hematopoietic progenitor cells in peripheral blood circulation. Exp. Hematol. 32(11), 1088-1096

165. Rodrigues-Moreira S., Moreno S.G., Ghinatti G., Lewandowski D., Hoffschir F., Ferri F., Gallouet A.S., Gay D., Motohashi H., Yamamoto M., Joiner M. C., Gault N., Romeo P. H. (2017). Low-dose Irradiation promotes persistent oxidative stress and decreases self-renewal in hematopoietic stem cells. Cell Press, 20(13), 3199-3211.

166. Parker F., White K., Phillips S., & Peckham M. (2016). Promoting differentiation of cultured myoblasts using biomimetic surfaces that present alpha-laminin-2 peptides. Cytotechnology, 68(5), 2159–2169.

167. Hommerding C.J., Childs B.G., Baker D. J. (2015). The role of stem cell genomic instability in aging. Curr. Stem Cell Rep. 1(3), 151-161

168. Aziz, A., S. Sebastian, and F.J. Dilworth (2012). *The Origin and Fate of Muscle Satellite Cells.* Stem Cell Reviews and Reports, **8**(2): 609-622.

169. Shelke S., Das B. (2015) Dose response and adaptive response of non-homologous end joining repair genes and proteins in resting human peripheral blood mononuclear cells exposed to gamma radiation. Mutagenesis.; 30: 365–379.

170. Toprani S.M., Das B. (2015). Radio-adaptive response of base excision repair genes and proteins in human peripheral blood mononuclear cells exposed to gamma radiation. Mutagenesis. doi: 10.1093/mutage/gev032.

171. Guedj A., Geiger-Maor A., Galun E., Benyamini H., Nevo Y., Elgavish S. h., Rachmilewitz J. (2016). Early age decline in DNA repair capacity in the liver: in depth profile of differential gene expression. Aging, 8(11), 3131–3146.

172. Sabin R, Pucci G, Anderson RM (2019). DNA damage processing is perturbed in both proliferative and non-proliferative cells of increased chronological cellular age. Rad. Res.; 192: 200-207.

173. Grudzenski S., Raths A., Conrad S., Rübe C. E., & Löbrich M. (2010). Inducible response required for repair of low-dose radiation damage in human fibroblasts. Proceedings of the National Academy of Sciences of the United States of America, 107(32), 14205–14210.

174. Blimkie M., Fung L., Petoukhov S…Klokov D. (2014). Repair of DNA Double-Strand Breaks is not modulated by Low-Dose Gamma Radiation in C57BL/6J Mice. Radiat. Res.; 181(5): 548-559.

175. Ikushima T. (1989). Radio-adaptive response: characterization of a cytogenetic repair induced by low-level ionizing radiation in cultured Chinese hamster cells. Mutat. Res., 227, 241-246.

176. Chen SL, Cai L, Meng QY, Xu S, Wan H, Liu SZ. Low-dose whole-body irradiation (LD-WBI) changes protein expression of mouse thymocytes: Effect of a LD-WBI-enhanced protein

RIP10 on cell proliferation and spontaneous or radiation-induced thymocyte apoptosis. Toxicol Sci. 2000; 55:97–106.

177. Wang Z., Sugie C., Nakashima M., Kondo T., Iwata H., Tsuchiya T., & Shibamoto Y. (2019). Changes in the Proliferation Rate, Clonogenicity, and Radiosensitivity of Cultured Cells During and After Continuous Low-Dose-Rate Irradiation. Dose-response; 17(2), 1559325819842733.

178. Yu X., Wang H., Wang P., Chen B. P., Wang Y. (2011). The Ku-dependent non-homologous end-joining pathway contributes to low-dose radiation stimulated cell survival. J. Cell Physiol., 226, 369-374

179. Zhao Y., Zhong R., Sun L., Jia J., Ma S., Liu X. (2015). Ionizing radiation-induced adaptive response in fibroblasts under both monolayer and 3-dimensional conditions. Plos One.; 10(3): e0121289

180. Yatagai F., Sugasawa K., Enomoto S., Honma M. (2009). An approach to estimate radioadaptation from DSB repair efficiency. J Radiat Res.; 50(5): 407–413